An-Najah National University

Faculty of Engineering & Information Technology

Continuous Solar Desalination Unit (CSDU): Design and Performance Investigation

Prepared by:

Lama A'raj

Reem Ashqar

Supervisor:

Eng. Mays Ali Shadeed

A Graduation Project Report Submitted to Energy Engineering and Environment Department in Partial Fulfillment of the Requirements for Bachelor Degree in Energy Engineering and Environment

Nablus, 2018

Acknowledgments

We would like to thank An-Najah National University for its financial support and provided everything to proceed with our project.

We wish to express also our gratitude to the excellent supervision provided by Eng. Mays Shadeed and her endeavor to make this work a success.

We are also indebted to Professor Amer El-Hamouz for his academic experience, support and patience during this work. God richly bless him and renews his strength and wisdom.

We wish to take this opportunity to thank the entire teaching staff of the energy and environmental engineering department for the wonderful work they are doing.

Last but definitely not the least; our utmost thanks go to the Almighty God, for giving us the strength, courage and direction to complete our project. Thanks to Our parents for the encouragement, support and prayers during this work, and our friends and colleagues for their immense support.

Table of Contents

List of Figures III

List of tables VI

Acronyms and Abbreviations VIII

Abstract IX

Chapter One: Introduction 1

Chapter Two: Desalination 4

2.1 Thermal processes: 6

2.1.1 Multi-Stage Flash Distillation 6

2.1.2 Multiple Effect Distillation 7

2.1.3 Solar Still 8

2.2 Membrane Processes 9

2.2.1 Reverse Osmosis 9

2.2.2 Electro-dialysis 9

Chapter Three: Solar still (SS) 10

3.1 Passive and active solar still: 11

3.2. Solar Still Enhancement Techniques 12

3.2.1 Basin (Absorber) 12

3.2.2 Glass 14

3.2.3 Other enhancements technology 16

3.3 Factors Affecting Solar Still Performance. 18

3.3.1 Environmental parameters 18

3.3.2 Design Parameters 19

3.3.3 Operational Parameters 20

Chapter Four: Methodology 21

4.1 Designing and Building Process 22

4.2 Investigation of CSDU Performance. 26

4.3 Measurements 29

Chapter Five: Results and Discussion.. 30

5.1 Evaporation Rate Measurements 30

5.1.1 Maximum and Minimum Evaporation Rate Achieved. 30

5.1.2 Comparison between Different Cases. 31

5.2 Environmental parameters affecting solar still performance 37

5.2.1 Effect of solar radiation. 38

4. Conclusion and Recommendation. 46

References.. 47

Appendices.. 50

List of Figures

Figure number	Name of the figure	Page number
Figure 2. 1	Multi-Stage Flash (MSF) process	6
Figure 2. 2	Multiple Effect Distillation Process	7
Figure 2. 3	MED- MVC Process	8
Figure 2. 4	MED- TVC Process	8
Figure 3. 1	The solar radiation distribution around the world	10
Figure 3. 2	A schematic diagram of single effect passive solar still	11
Figure 3. 3	A schematic diagram of single effect active solar still	12
Figure 3. 4	Pictorial view of Spherical Solar Still	13
Figure 3. 5	Schematic view of tubular solar still	13
Figure 3. 6	A schematic diagram of multi effect passive solar still	14
Figure 3. 7	Schematic view of hemispherical solar still	15
Figure 3. 8	Schematic view of pyramid solar still	15
Figure 3. 9	Classifications of PCMs	16
Figure 3. 10	A photo of the modified stepped solar still	17
Figure 3. 11	The variation of solar intensity and still output	18
Figure 3. 12	The effect of the variation of evaporation area on distillation yield	19
Figure 3. 13	The effect of water depth on the solar still productivity	20
Figure 4. 1	Schematic diagram of designed solar still using AutoCAD	22
Figure 4.2	Thermal camera pic for the unit (a): before insulation, (b): after insulation)	25

Figure 4. 3	(a) - 3D image for CSDU, (b) - photograph for CSDU with condenser	26
Figure 4. 4	A satellite photograph of ANNU, CSDU location is pointed with a green arrow	27
Figure 5. 1	The accumulative volume for Maximum and minimum cases	30
Figure 5. 2	Comparison between case-1 and case-2 at SRavg = 5.37 kWh/ m2.day, Tamb-avg = 22.12 C^{o} and RHavg = 39.33%	32
Figure 5. 3	Comparison between case-2 and case-3 at SR = 5.878 kWh/ m2.day, Tamb = 24.8 C^{o} and RH = 34%	33
Figure 5. 4	Comparison between case-1 and case-4 at SRavg = 5.457 kWh/ m2.day, $Tamb_{-avg}$ = 28.88 and RH_{avg} =24.11%	33
Figure 5. 5	Compare between case-1 and case-5 at Sr = 6.27 kWh/m2.day, Tamb = 25.8 C^{o} and RH = 25.8%	34
Figure 5. 6	A comparison between all cases that described in table-4.3	35
Figure 5. 7	Variation of hourly evaporation rate with solar radiation on 24/4/2018	36
Figure 5. 8	Variation of solar intensity on two different days	37
Figure 5. 9	The effect of solar radiation on unit's productivity for 15/3/2018	37
Figure 5. 10	The effect of solar radiation on unit's productivity for 27/3/2018	38
Figure 5. 11	Relationship between solar radiation and daily flux	38
Figure 5. 12	Relationship between daily flux and temperature	39
Figure 5. 13	Temperature variation with solar radiation for 2/4/2018	40
Figure 5. 14	Temperature variation with solar radiation for 4/4/2018	40
Figure 5. 15	Temperature variation between the inside and outside the basin for 2/4/2018	40
Figure 5. 16	Diurnal variation of relative humidity and ambient temperature on 4/4/2018	41

Figure 5. 17	Relationship between relative humidity and evaporation flux	42
Figure 5. 18	Effect of solar radiation and relative humidity on Daily flux	43
Figure 5. 19	Variation of inlet and outlet relative humidity for 4/4/2018	44
Figure 5. 20	Incandescent bulbs represent the energy consumption of CSDU	44

List of Tables

Table number	Name of the figure	Page number
Table 2. 1	Available Water Quantity in Palestine by Region and Source	4
Table 2. 2	Quantity of Water Supply for Domestic Sector and Daily Allocation per Capita in Palestine by Region and Governorate, 2014	5
Table 4. 1	Previous investigations on various Solar Stills design and performance	21
Table 4. 2	Description about CSDU components	23
Table 4. 3	Site location and weather conditions for Nablus	26
Table 4. 4	Operating conditions for each case	28
Table 5. 1	The ambient conditions for maximum and minimum evaporation rate	31
Table 5. 2	Accumulative volume for all mentioned cases	35
Table 5. 3	The reduction in evaporation flux for each comparison case.	36
Table 5. 4	The evaporation fluxes at average weather conditions for all conducted experiments.	37
Table 5. 5	Daily flux and average solar radiation	40
Table 5. 6	Daily flux and Ambient Temperature	41
Table 5. 7	Daily flux and Relative Humidity	44
Table 5. 8	Daily flux, relative humidity and solar radiation for each day	44

List of Appendices

Appendix	Description	Page
Appendix A	Datasheets	49
Appendix B	Calculations	51
Appendix C	Experimental Results	53

Acronyms and Abbreviations

CSS	Conventional Solar Still
ED	Electro- dialysis
FSS	Fan Solar Still
MED	Multiple-Effect Distillation
MSF	Multi- Stage Flash
MVC	Mechanical vapor compression
PCM	Phase Change Material
PV	Photovoltaic
RH	Relative Humidity
RO	Reverse Osmosis
SR	Solar Radiation
SS	Solar Still
Tamb	Ambient Temperature
TVC	Thermal Vapor Compression

Abstract

Desalination techniques –to remove salts from water – have been used widely around the world, to reduce the water crisis, since there are nearly 1 in 10 people lack access to safe water. Solar desalination is one of the most promising technique among all of other desalination techniques especially in remote areas that suffer from lack of fresh water.

Most of the available solar designs are batch which gave commonly low productivity, therefore, this project aims to design and build a continuous solar desalination unit (CSDU), and study the effect of environmental and operational conditions on its productivity where rotating belt, suction fan and compressor were added and classified into five cases.

The solar still has been experimentally tested for three months. Promising results were achieved, the productivity was measured along several days during February to April. The maximum and minimum evaporation fluxes achieved were 11.4 and 6.9 (liter/m^2.day), respectively, while solar irradiation at those days were (5.03 and 4.11kWh/m^2.day), respectively. The average productivity for conventional solar stills was (3-4) liter/ m^2.day, which lower than CSDU's average productivity that reach approximately 9.73 liter/ m^2.day, where 64.02% enhancement is obtained.

The tested results confirmed that running the apparatus with rotating belt, compressor, and fans at average solar radiation= 5.65kWh/m^2 has a high significant effect than running the unit while they are turned off. The improvement was 86%, which mean that integrating of these enhancements will improve the productivity of solar still.

In addition, results indicate that the evaporation rate was highly affected by weather conditions. Since the evaporation rate increases with increasing solar radiation and temperature and decreases with increasing the relative humidity. These prove that the constructed apparatus is working in the right way.

Chapter One: Introduction

Access to clean drinking water is one of the most important international health issues today. It is expected that by the year 2025, 1/4 of the world population will be affected by water scarcity, and 2/3 will experience water-stressed conditions. By 2030, 1/2 of the world population will experience high water stress[1]. The rapid growth of population and the enormous need for water in many sectors caused shortage of the fresh water all over the world. Only less than 1% of the water is available for the society for direct use[2].

Desalination is one of the most appropriate solutions to overcome the water shortage problem, which is defined as the process of removing the dissolved solids such as salts and minerals from water to obtain potable water with low salinity and high quality. Desalination technologies are classified based on the separation process adopted either thermal or membrane. Thermal process includes multi-stage flash (MSF), multiple-effect distillation (MED), mechanical vapor compression (MVC), and solar still (SS). Whereas membrane process includes reverse osmosis (RO) and electro dialysis (ED) [3] . However, these technologies are not appropriate for remote villages and small islands. Large amount of energy is needed for these methods [4].

The performance of a solar still may be quantified by efficiency and productivity. Efficiency is defined as the ratio of latent heat energy of the condensed water to the total amount of solar energy incident on the still. Whereas, productivity is the water output per area of solar still per day[1].

Solar still technology basically consists of basin covered with a transparent glass cover, which allows the solar radiation to enter and evaporate the saline water inside the basin by green house effect. It is normally painted with black color to absorb maximum solar heat. The water vapor produced is condensed as droplets of fresh water, then fresh water is collected [5].

This design is considered as conventional basin type solar still. However, it has several drawbacks due to its low productivity. Generally, thermal efficiency of conventional solar still is around (35%-40%) with normal daily productivity of 3-4 L/m^2.day [6] .

Many modifications were made to improve this method. Arunkumar et al. [7] addressed solar stills of various configurations in different designs, his experiential study included testing seven solar stills designs during January to May 2011, operated in the same conditions. These configurations are spherical solar still, pyramid solar still, hemispherical solar still, double basin glass solar still; concentrator coupled single slope solar still, tubular solar still and tubular solar still coupled with pyramid solar still. Their performance evaluations in converting brackish water into fresh water for drinking are presented. The results showed that the compound parabolic concentrator-assisted tubular solar still shows the max yield.

Hitesh et al. worked on three enhancing methods like use of fins, energy storage materials and multi-basin solar still. The results were concluded as followed. Firstly, integration of fins in the basin plate increase the basin exposure area and thus lead to higher evaporation rate. Secondly, energy storage materials like sponges with pore holes where used to store energy. Finally, multi-basin solar still utilizing latent heat of lower basin to increase the evaporation rate in upper basin [8].

There is a lot of scope of researchers work on the solar still and its various designs to enhance its productivity. Al-Karaghouli and Alnaser investigated the performances of single and double basin solar-stills, which was performed in the Kingdom of Bahrain. Stills were with the same basin area, each still inners diameter was (90m×50 m) considering many factors for two cases, with insulations and without insulations. Based on experimental results, the double basin still showed better results in distillate production, and for the influence of side's insulation on water production [9].

Omara et al. [10] reported the benefits of using water fan inside a conventional solar still (CCS) where two stills CSS and Fan solar still (FSS) were constructed and tested. Wind turbine was used to operate the water fan; they found that the maximum productivity of FSS is achieved at water depth of 1 cm for fan rotational speed less than 22rpm and at 3cm for speeds greater than 22 rpm with fan efficiency about 39.8 %.

Kaviti et al. [5] discussed various designs of inclined solar stills. The productivity can be enhanced by inclining the basin at an angle depending on altitude of the place and season.

A stepped solar still was investigated by [30] to overcome the problem of obtaining the minimum water depth with and without modifications include adding of fins, reflector and external condenser. The daily productivity before and after modifications was 6.9 kg/m^2, 8.9 kg/m^2 respectively.

Some studies have been performed using continuous solar desalination process. El-ajouz [11] presents a modification of stepped solar still with continuous water circulation using a storage tank for sea and salt water. The results indicate that, the productivity of the modified stepped still is higher than that for conventional still approximately by 43% and 48% for sea and salt water with black absorber respectively, while 53% and 47% of sea and salt water, respectively with cotton absorber. And in another paper for El-ajouz [12], he conducted a theoretical study of the performance evaluation of a continuous water flow inclined solar still desalination system is performed. Three models are studied for inclined solar still desalination system with and without water close loop. The effects of the water mass, water film thickness, water film velocity and air wind velocity on the performance of the three models are studied. The results show that the inclined solar still with a makeup water is superior in productivity (57.2% improvement) compared with a conventional basin-type solar still.

Sharshir et al. [3] discussed in his study many factors affecting solar still productivity. Increasing of solar intensity, glass-water temperature difference, free surface area, inlet water temperature, glass-cover with high thermal conductivity and solar still insulation which 80% of productivity could be achieved by selection of appropriate insulation. All of these parameters are directly proportional with solar still productivity. Whereas, water deepness and glass thickness are inversely proportional with still productivity. Also Hitesh and patel [4] discussed the most important factors include climate parameters such as wind velocity, ambient temperature and solar radiation. In addition, design parameters, such as water depth, glass thickness and cover inclination.

Most of the studies conducted previously have used batch desalination processes. To the best knowledge of the authors, few studies were conducted on designing continuous solar desalination system. Investigating the continuous solar desalination process is of great importance to the industry. Therefore, the main goal of this project is to investigate the inclined solar still under continuous operation conditions. To achieve this goal a continuous desalination using solar energy will be designed and tested. The effect of various parameters such as air velocity and direction, motor speed, weather conditions and preheating of feed water on the desalination process will be investigated.

Chapter Two: Desalination

Although water seems to be super-abundant natural resource on the planet earth. Fresh water makes up a very small fraction of all water on the planet. While nearly 70% of the world is covered by water, only 2.5% of it is fresh. The rest is saline and ocean water. Even then, just 1% of fresh water is easily accessible, with much trapped in glaciers and snow fields [2, 13]. This is due to rapid increase in population and unequally distribution of water among the world. Some regions are rich with fresh water, whereas others suffer from chronic lack of potable water.

Palestine is considered as a rich region in water resources. However, it faces a fresh water shortage; due to Israel policy which is based on taking control of water resources and preventing Palestinians from using it. Total available water quantity in Palestine reach 342.7 million m^3 in 2014 divided into four resources described in table-1 [14] .Where quantity of water supply for domestic sector appear in table-2 [14]

Therefore, desalination was an alternative solution to facilitate the fresh water accessibility and overcome some of these obstacles. There is about 4.7 million m^3/ year of desalinated drinking water in Palestine [14].

Table 2. 1: Available Water Quantity in Palestine by Region and Source [14]

Unit: Million m^3/Year

Region	Source			المصدر	Total
	Water Purchased from Israeli Water Company (Mekorot)	Desalinated Drinking Water	Springs Discharge	Water Pumped from Palestinian Wells	
Palestine	**63.5**	**4.7**	**28.2**	**246.3**	**342.7**
West Bank*	60.0	-	28.2	75.6	**163.8**
Gaza Strip	3.5	4.7	-	170.7	**178.9**

*Data doesn't include those parts of Jerusalem which was annexed forcefully by Israel following its occupation of the West Bank in 1967.

Table 2. 2: Quantity of Water Supply for Domestic Sector and Daily Allocation per Capita in Palestine by Region and Governorate, 2014 [14]

Region /Governorate	Daily allocation per capita (Liter/capita/day)	Total Losses (Milion m^3)	Quantity of water consumed (Milion m^3)	Quantity of water supply (Milion m^3)
Palestine	**79.4**	**65.0**	**126.3**	**191.3**
West Bank	**79.1**	**28.6**	**74.2**	**102.8**
Jenin	39.2	2.0	4.4	6.4
Tubas	55.9	0.7	1.3	2.0
Tulkarm	66.8	2.7	4.4	7.1
Nablus	64.7	3.1	8.9	12.0
Qalqiliya	165.2	2.0	6.6	8.6
Salfit	90.1	0.8	2.3	3.1
Ramallah & Al-Bireh	125.3	2.4	15.7	18.1
Jericho & Al Aghwar	213.0	1.9	4.0	5.9
Jerusalem*	40.0	2.1	2.3	4.4
Bethlehem & Hebron	73.3	10.9	24.3	35.2
Gaza Strip	**79.7**	**36.4**	**52.1**	**88.5**
Gaza North	90.1	11.7	11.7	23.4
Gaza	75.6	10.0	17.0	27.0
Deir Al-Balah	87.4	5.4	8.3	13.7
Khan Younis	73.3	5.7	9.0	14.7
Rafah	75.4	3.6	6.1	9.7

*Data doesn't include those parts of Jerusalem which was annexed forcefully by Israel following its occupation of the West Bank in 1967.

Desalination is a widely used method to get pure water using several processes. These processes as R. Bharadwaj et al. classified into two types. The first one is thermal processes such as Multi-stage effect (MSF), multiple effect distillation (MED) and solar still (SS), and the second one is membrane processes include reverse osmosis(RO) and electro-dialysis(ED).These two types explained in section 2.2 ,2.3, respectively [13].

2.1 Thermal processes:

2.1.1 Multi-Stage Flash Distillation

MSF process involves the use of distillation through several multi-stages chambers. Feed water, which introduced is heated using brine heaters. Then the heated water enters the first chamber where there is low pressure. Since the entering water's temperature is higher than the boiling point temperature at vacuum pressure (low pressure). A part of the water flashes to steam. Remaining brine enters multiple stages where the process repeats. Moreover, this increase the quality of water produced. Before entering brine heaters, brine water enters condensing coils located inside the chambers in order to preheat the incoming brine. In addition, these condensing coils are used for condensing the evaporated water, and then pure water is collected as shown in figure-1.

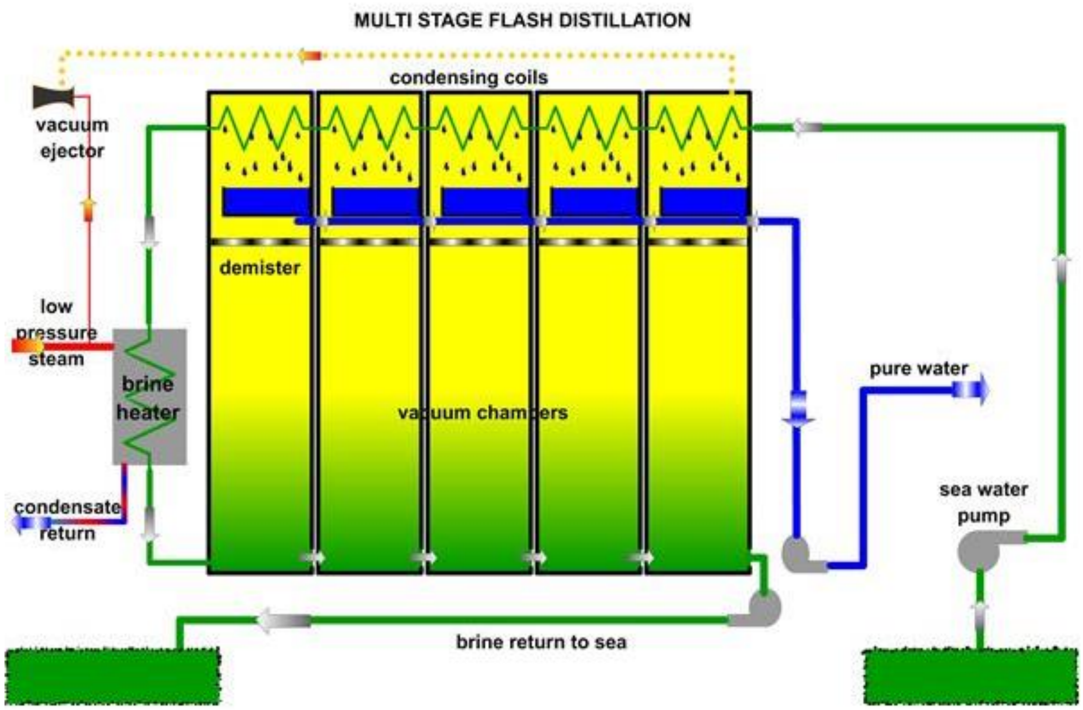

Figure 2. 1 : Multi-Stage Flash (MSF) process [15]

2.1.2 Multiple Effect Distillation

MED process occurs in a series of vessels called evaporator effects. Each maintained at lower pressure and temperature than the last. It differs from MSF that steam is introduced inside the tubes. Since tubes are cooled when it spraying with seawater as shown in figure-2. Steam condenses inside the tubes to distilled water. At the same time, sprayed water evaporates due to latent heat of condensation. This vapor can be used as heating media for the next effects, where decreasing pressure cause water evaporates at lower boiling point. Additional amount of vapor will be released at lowering pressure, which will condense into distilled inside the next effect. This process is repeated in a series of effect to make a multiple effect distillation.

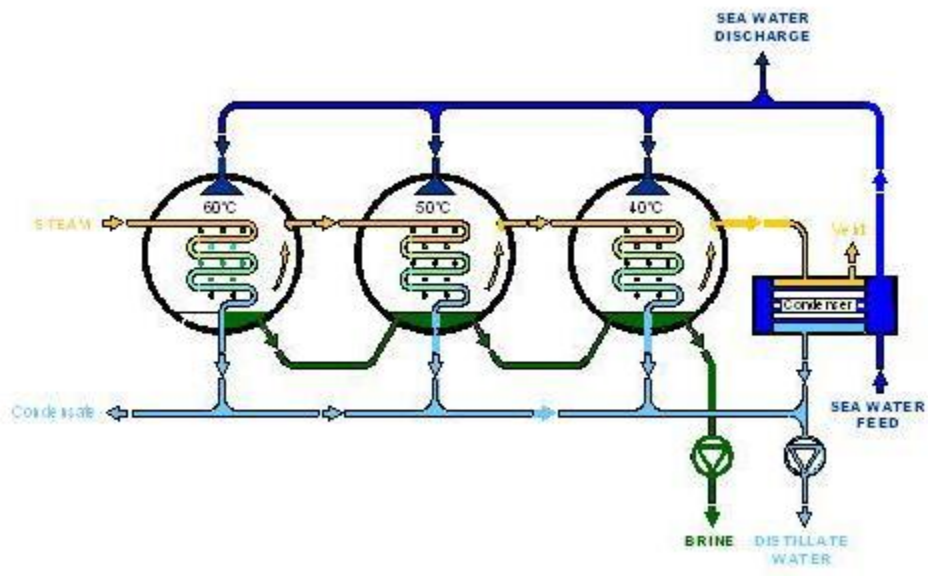

Figure 2. 2: Multiple Effect Distillation Process [16]

To enhance MED process, vapor can be compressed in two methods: Mechanical (MED-MVC) and thermal compression (MED-TVC). Figure-3 show MED-MVC process, it uses only electrical energy to drive a centrifugal compressor. The compressor allows the vapor to be recycled from the cold effect and uses in the hot one. Whereas MED-TVC using a thermo compressor between one of the effect and the hot one as shown in figure-4.

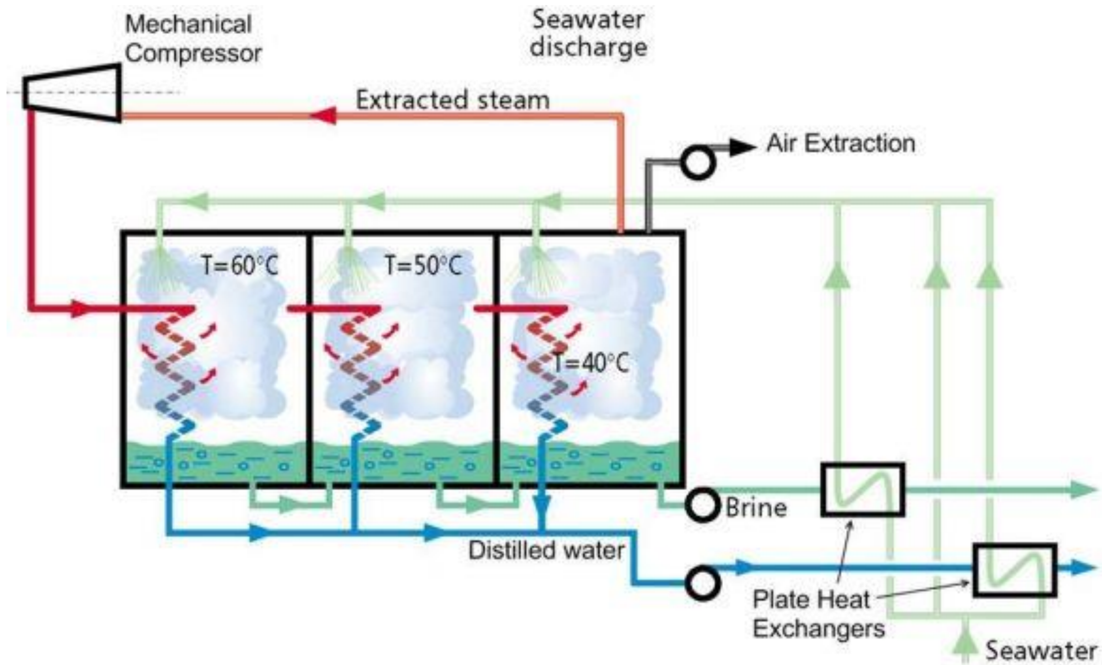

Figure 2. 3: MED- MVC Process [16]

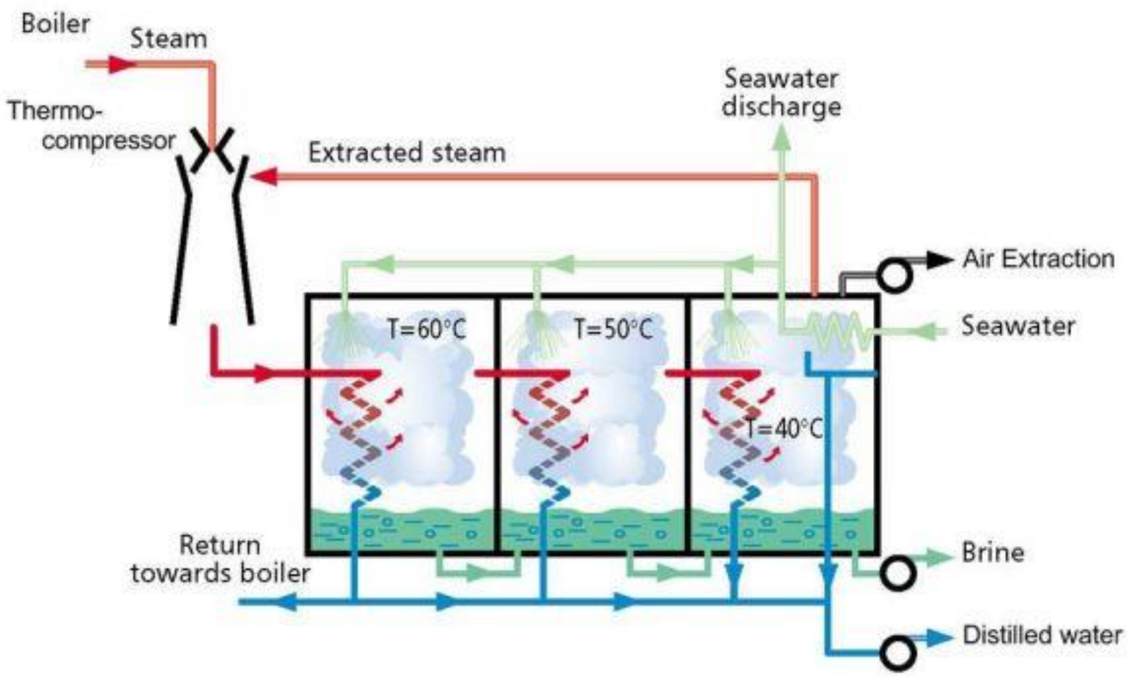

Figure 2. 4: MED- TVC Process [16]

2.1.3 Solar Still

Solar Still is one of the most promising thermal techniques. More details can be found in chapter 3.

2.2 Membrane Processes

2.2.1 Reverse Osmosis

RO is the most widely used in membrane processes. In the RO process, water from a pressurized saline solution is separated from the dissolved salts by flowing through a water-permeable membrane. The permeate (the liquid flowing through the membrane) is encouraged to flow through the membrane by the pressure differential created between the pressurized feed water and the product water, which is at near-atmospheric pressure. The remaining feed water continues through the pressurized side of the reactor as brine. No heating or phase change takes place. As the product, water passes through the membrane, the remaining feed water and brine solution becomes more and more concentrated. To reduce the concentration of dissolved salts remaining, a portion of this concentrated feed water-brine solution is withdrawn from the container. Without this discharge, the concentration of dissolved salts in the feed water would continue to increase, requiring ever-increasing energy inputs to overcome the naturally increased osmotic pressure[17].

2.2.2 Electro-dialysis

ED is an electrochemical process for the separation of ions across charged membranes from one solution to another under the influence of an electrical potential difference used as a driving force. This process has been widely used for production of drinking and process water from brackish water and seawater, treatment of industrial effluents, recovery of useful materials from effluents and salt production[18]

A large amount of power is needed to operate such these processes. Fossil fuel is one of the main sources to provide this power. However, it is considered as one of the main producers of CO_2 emissions, which will lead to an increase in greenhouse gases and environmental pollution. Switching from depending on fossil fuel to utilizing the power of Renewable energy is one of the best solutions. Solar energy is one of the RE sources that can be used directly as a heat source in solar still.

Chapter Three: Solar still (SS)

Investments in solar energy are now rapidly growing in the world as an alternative solution instead of using fossil fuel. Due to high costs of energy production and the need for addressing the increasing demand on energy, solar energy is going to be the competitive and future energy source. The amount of solar energy incident on a geographical location is considered as one of the most important factors determining the applicability of using this type of energy.

The solar energy, which reaches the earth's surface, is approximated by 1.08×10^{18} kWh, if one ten thousandth of the total solar energy used in producing energy, the global energy demand will be covered. The figure below shows the solar radiation distribution around the world.

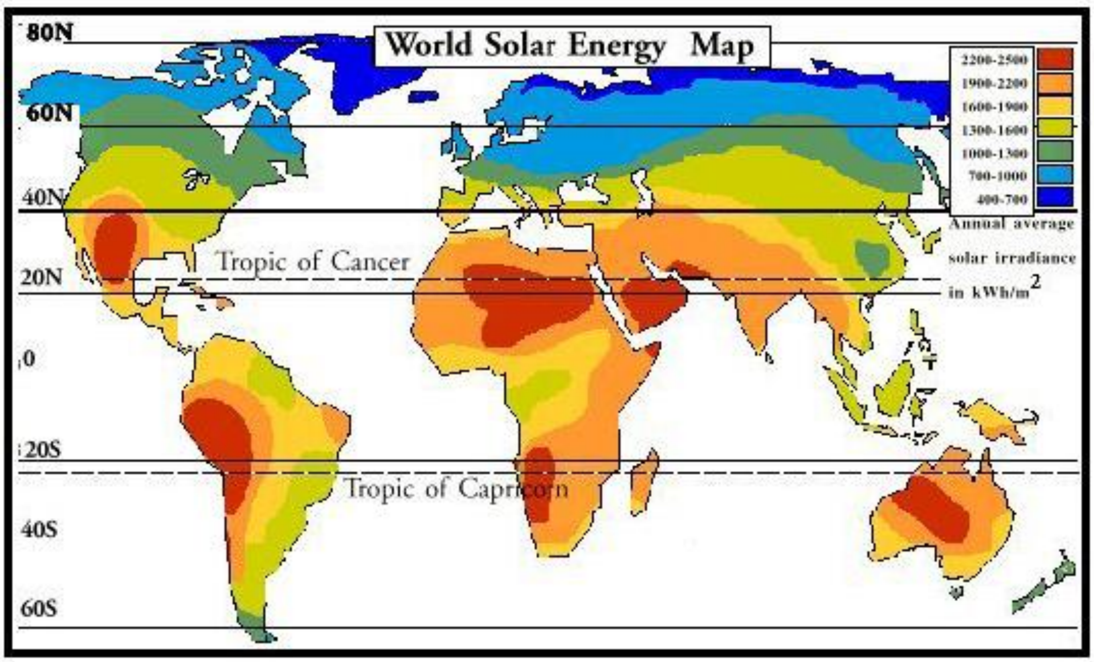

Figure 3. 1: The solar radiation distribution around the world [19]

In Palestine, there is high potential for solar energy that helps in promoting the use of solar energy in many applications such as water heating, water desalination and producing electricity in remote locations isolated from the electrical networks. Palestine receives about 3,000 hours of sunshine per year and has an average solar radiation of 5.4 kWh/m2 daily [20].

SS is a thermal desalination technique used to get distilled water by using solar energy as the main power source. Moreover, the dependency on solar energy and the need for less fossil fuel makes it a good solution to be used in remote and arid areas with portable water shortage. Where there is an urgent need to access fresh and clean water in an effective way, with a relatively low cost and environmentally friendly technique.

The conventional solar still (CSS) mainly depends on evaporation and condensation in natural way, where solar radiation passes through a transparent glass cover, to heat the water at the basin, then the evaporation start. Then the evaporated water is condensed in the glass cover to get pure water.

The condensation on the glass cover is considered as one of the main disadvantages of this technique since the water droplets form district the solar radiation. The thermal efficiency for CSS is around (35-40 %) with normal daily productivity of (3-4 L/m^2.day) [10], which is considered very low compared with other thermal desalination process. These drawbacks motivate researchers to improve S.S, and optimizing its design to increase its productivity through enhancing evaporation and condensation rate using heat storage and by reducing thermal losses.

3.1 Passive and active solar still:

Passive solar still is classified into two categories according to operation mode: passive and active SS. For passive SS, the source of heat to evaporate saline water is directly through the sun. While active SS, an external source can be used like pumps, fans, PV and solar heaters, which are coupled to the still.

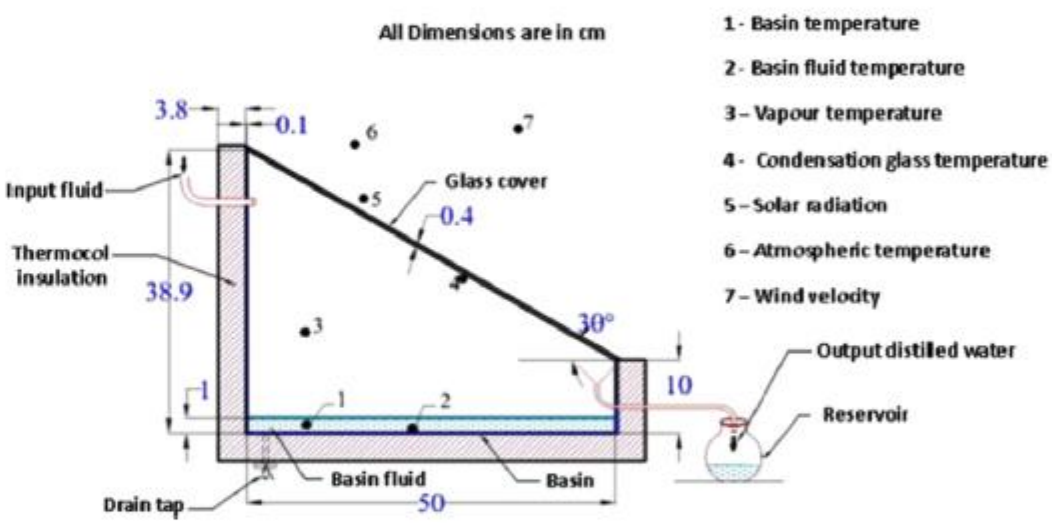

Figure 3. 2: A schematic diagram of single effect passive solar still [5]

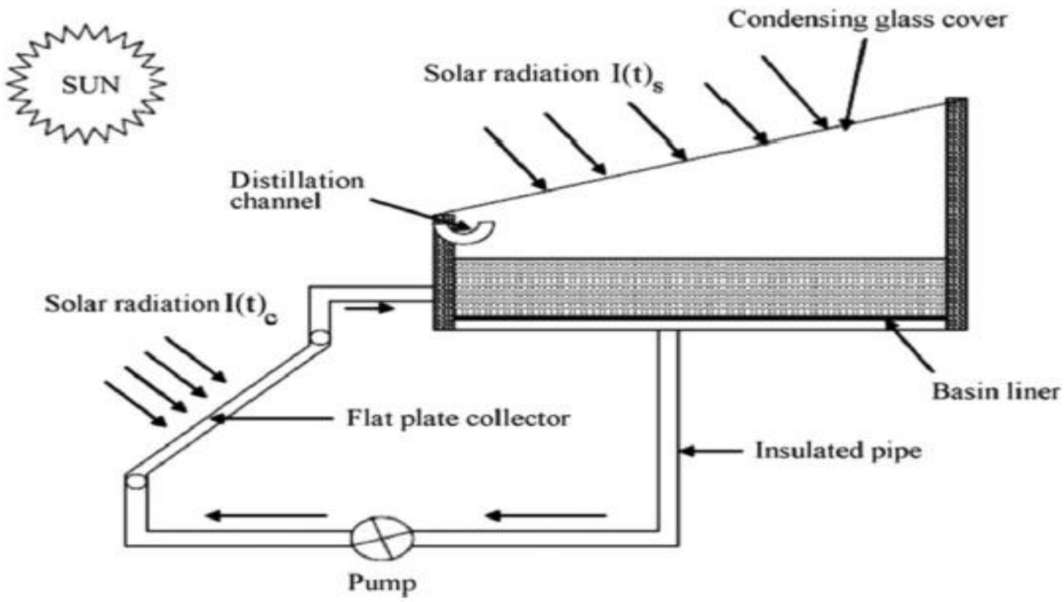

Figure 3. 3: A schematic diagram of single effect active solar still [5]

3.2. Solar Still Enhancement Techniques

SS efficiency can be enhanced utilizing various techniques and several parameters affecting its productivity. Most of the studies investigate these techniques on solar still components that will be discussed in the next sections.

3.2.1 Basin (Absorber)

The basin is considered as an absorber for the SS. It can be shaped as rectangular, which is common one, hemispherical or tubular, which are shown in figure 7 and 8, respectively. Moreover, absorber can be horizontal or inclined which is considered as one of the enhancement technique. The concept of inclined solar still based on the fact that, larger evaporation surface area and an efficient angle to the sun, which in turns lead to increase the amount of distilled water. Kumar kaviti et al. reviewed the most important parameter influencing the productivity. In this study, they concluded that the inclination could enhance the productivity. In addition, the basin can be single, double or multi layers figure 9. More layers improve SS efficiency by utilizing the dissipated latent heat.

Figure 3. 4: Pictorial view of Spherical Solar Still [7].

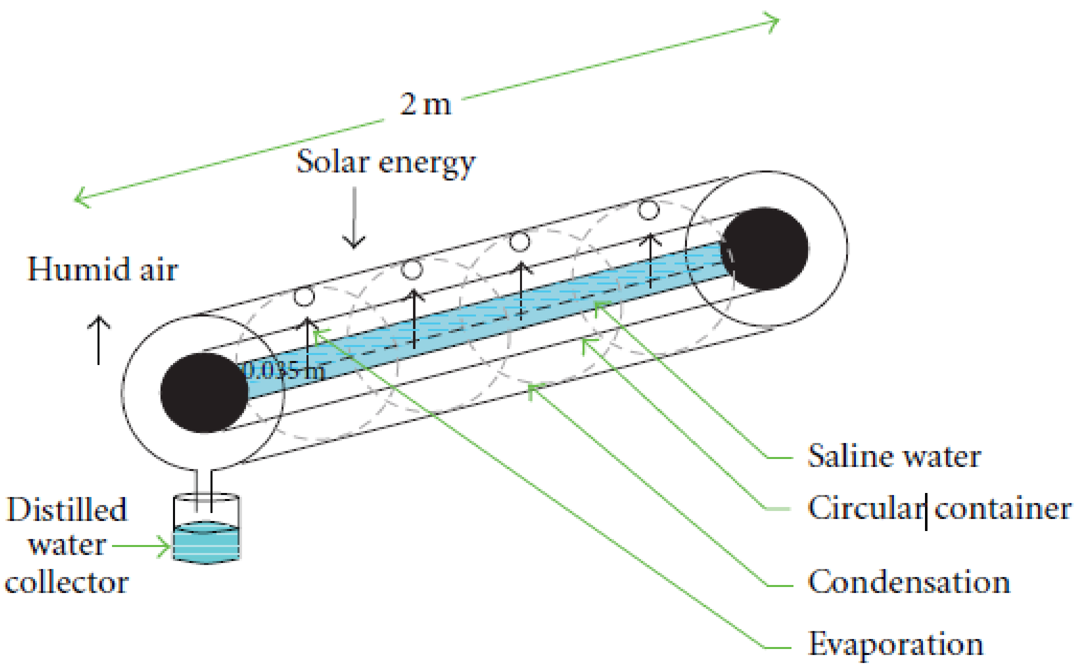

Figure 3. 5: Schematic view of tubular solar still [7].

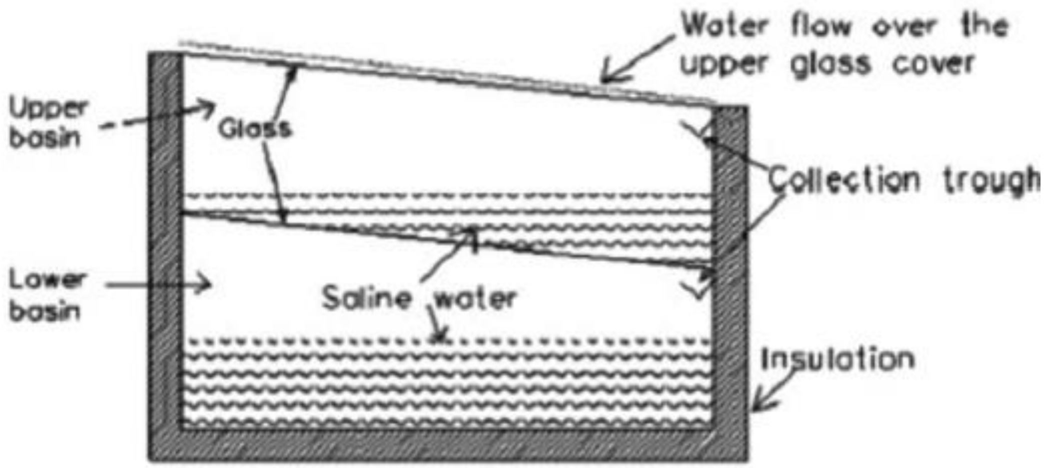

Figure 3. 6: A schematic diagram of multi effect passive solar still [21]

Furthermore, absorbing and storage materials acts as a good enhancer for still basement. Wick materials such as sponge, cotton and jute cloth are commonly used in many experimental works. Sengar et al. [22] conducted an experiment using black cotton to improve the evaporation rate and increase in productivity of SS by 12%. Black painted and asphalt is a simple and cheap way to improve basin absorptivity.

3.2.2 Glass

Glass is the transparent cover that should be air tightness and has low reflectivity. Incident solar radiation passes through it to heat basin saline water, then vapor condensation takes place. So cleaning glass cover continuously increasing solar transmission therefore, increasing SS performance.

Glass cover can be find in different shapes. It can be single or double slope, hemispherical figure 10, pyramid figure 11 or tubular. Glass plays an important role in condensation process. The cover should be inclined toward the best orientation where inclination angle equal to the latitude of the place. The thickness should be low as possible to increase the transmissivity[16].

Glass temperature is an important parameter that affect solar still yield. This can be achieved in several cooling ways via water film or fan to provide airflow over the glass to enhance the condensation process. The need for cooling comes from high temperature inside the basin due to greenhouse effect, which cause high glass cover temperature.

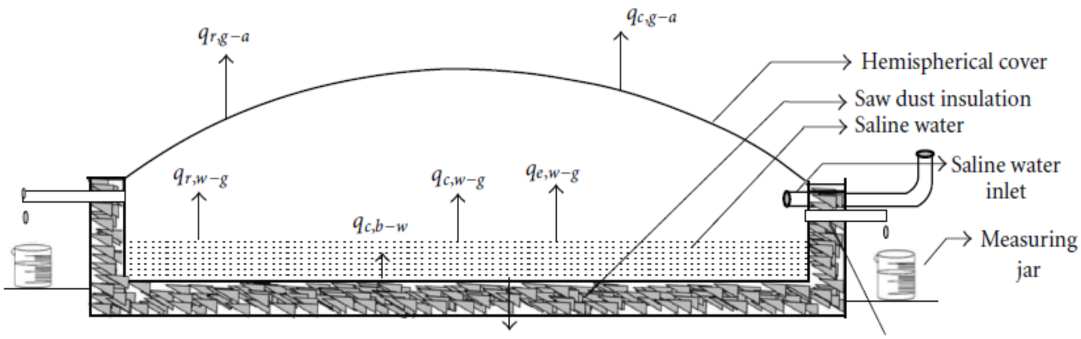

Figure 3. 7: Schematic view of hemispherical solar still [7]

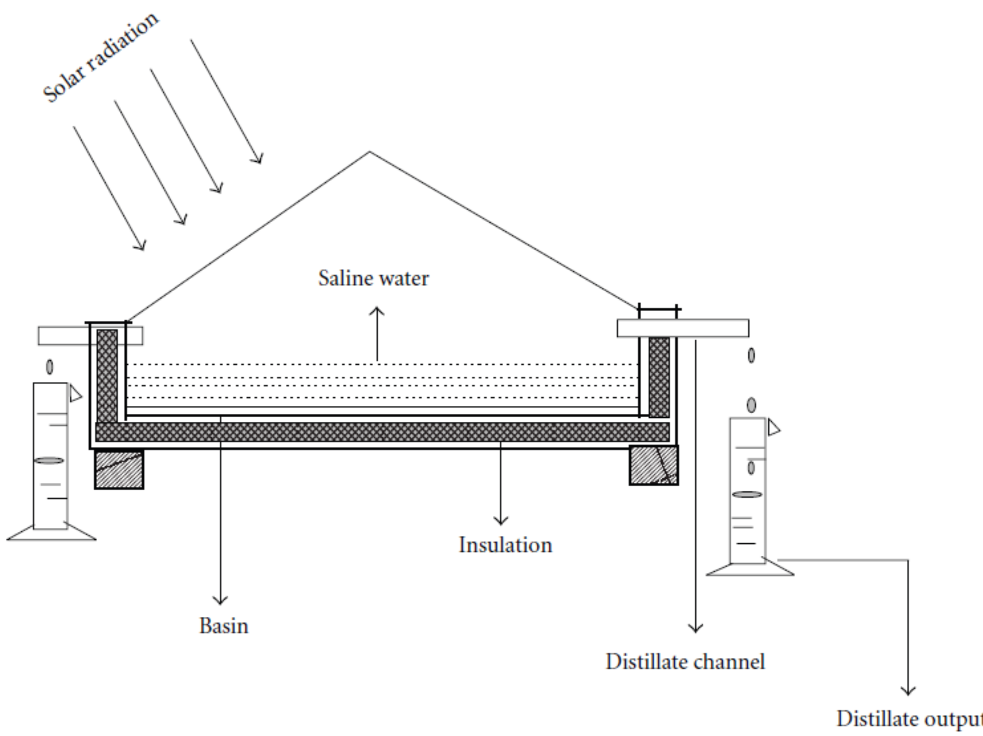

Figure 3. 8: Schematic view of pyramid solar still [7].

3.2.3 Other enhancements technology

Phase change material (PCM) is a storage material using in the basin as an enhancement technique. It depends on melting and freezing principle, where it absorbs heat during sunny days and change its phase to liquid form. Then release it during the night and cloudy days and backs to its original solid phase. PCMs stores 5-14 times more heat per unit volume, unlike sensible thermal energy storage materials such as masonry or rocks [23].

PCM classified into three categories: Organic, inorganic and eutectic as shown in figure [12]. Organic compound includes paraffin wax, easters, acids and alcohols that used for household application. Where salty hydrates are the most well-known inorganic PCMs. While eutectic is a mix of organic and inorganic PCMs.

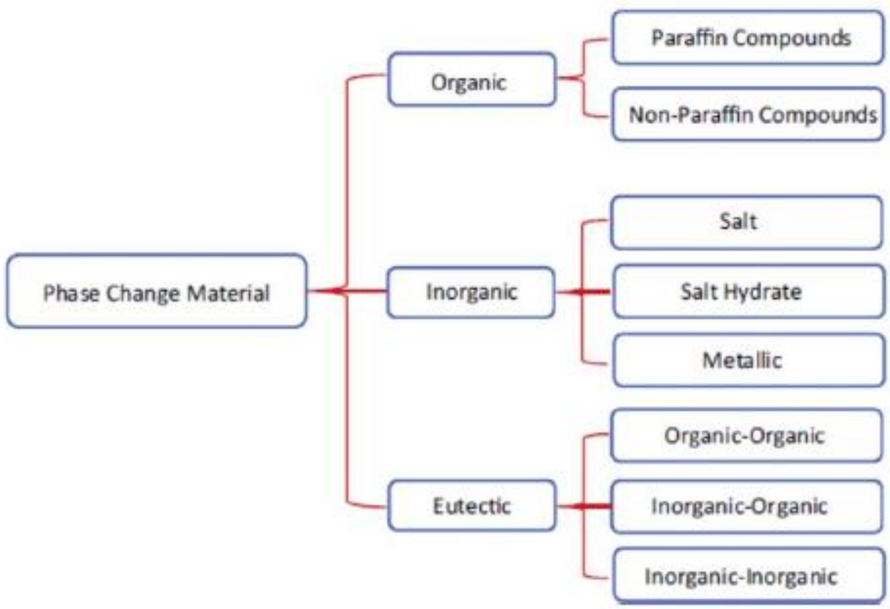

Figure 3. 9: Classifications of PCMs [24]

Condensers is an external device used to aggregate the evaporated water, then condensate it in an efficient way better than natural condensation inside the still itself. It has been found that the productivity increased after adding an external condenser by about 70-75 against the CSS [25].

Another modification to enhance the thermal performance of solar still is **reflectors** either external or internal. Reflectors concentrate or radiant large amount of solar radiation. Moreover, it is more practical in places where solar radiation is weak and the ambient temperature is relatively low. Besides, it decreases the waste heat energy from the SS.

A modified stepped solar still with internal and external reflectors (figure 3.10) was investigated by Omaro.et al. He concluded that the modified SS performance enhanced by 125% more than CSS [3].

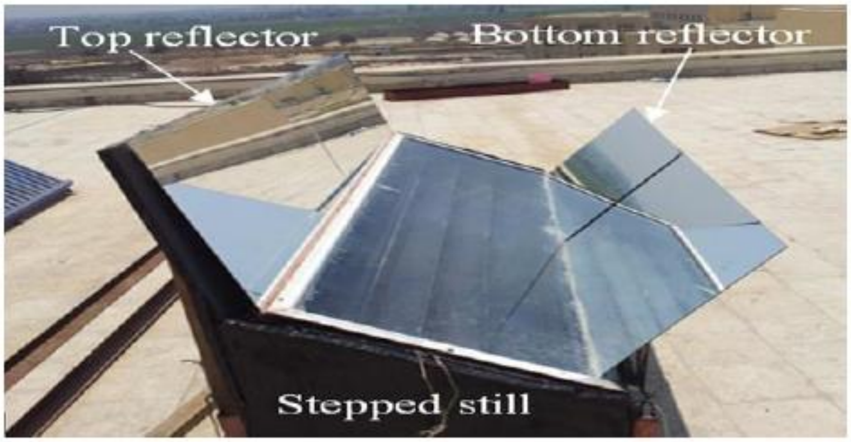

Figure 3. 10: A photo of the modified stepped solar still [3]

In addition, one of the significant improvements is **fins** attached with still basin. Integration of fins allows much exposure area, which in turns increase the heat transfer rate.

Naggar conducted an experimental work to compare between the SS with finned surfaces alternatively, without. The results showed that the efficiency of the finned surface was 55.3%, while it was 42.36% in non-finned surface of the still [26].

Fins can be found in various shapes: spherical, helical, rectangular or square fins. It can be aluminum or stainless steel, however aluminum fins has higher productivity than stainless steel [27].

3.3 Factors Affecting Solar Still Performance.

There are different parameters affecting S.S productivity. They are classified to environmental, design and operational parameters as Abujazar et.al. classified it [28].

3.3.1 Environmental parameters

Solar still productivity influence highly by environmental parameters because its metrological factors are unpredictable. These factors include solar intensity, ambient temperature, relative humidity and wind velocity.

The **intensity of solar radiation** is the most metrological factor affecting solar still positively. Increasing solar radiation, Increases temperature difference between glass and water, which increase the operation process [3, 4, 28]. Figure-16 shows the relationship between solar intensity and SS productivity.

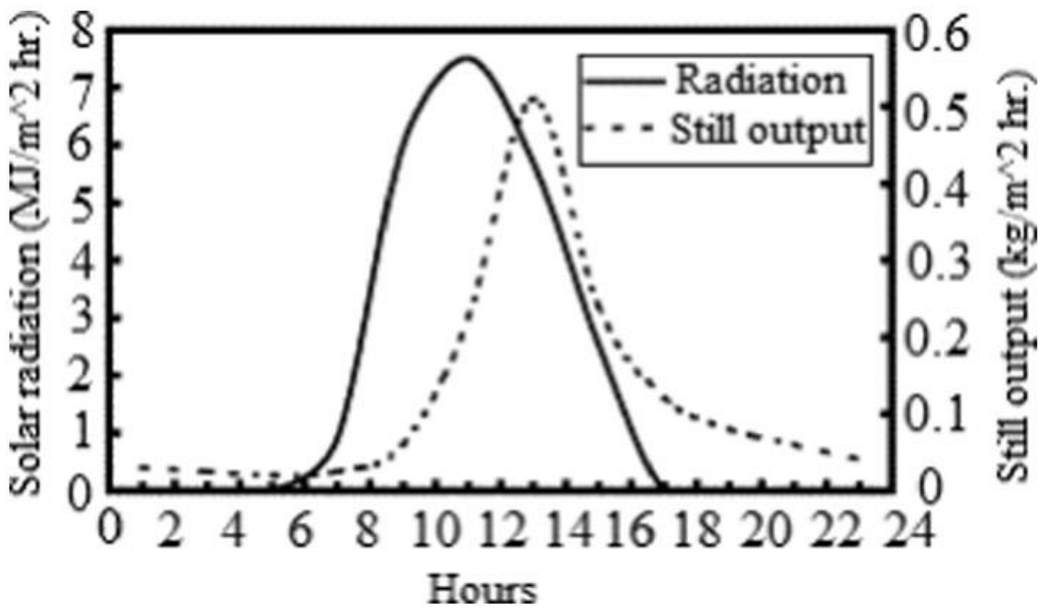

Figure 3. 11: the variation of solar intensity and still output [28]

Air temperature is considered as one of climatic parameters that affect the performance of solar still. Ambient temperature affect condensing glass cover, which will affect temperature difference between glass cover and water. Moreover, ambient temperature is affected by solar radiation [3, 4, 28].

The effect of relative humidity from previous studies has not been extensively studied. This is because no air enters the device to affect its inside relative humidity. At variance of CSDU that uses a fan to increase the driving force in the unit, which will highly affected the humidity inside the solar still.

For the **wind velocity**, it is directly proportional to SS productivity. The increasing in wind speed causes an increasing in convicted heat transfer from the cover to the atmosphere, and consequently increase glass-water temperature difference. The performance of SS increases with increasing wind speed up to a certain velocity [3,4, 28].

3.3.2 Design Parameters

There are different design parameters affect SS productivity rate, which can be controlled and designed. These parameters include evaporation area, water depth and insulation.

The **exposure evaporated surface area** is directly proportional to water evaporation rate in SS, where larger surface area leads to evaporation to increase as shown in figure-15. For achieving this, fins, sponges and wick types can be used at the basin water.

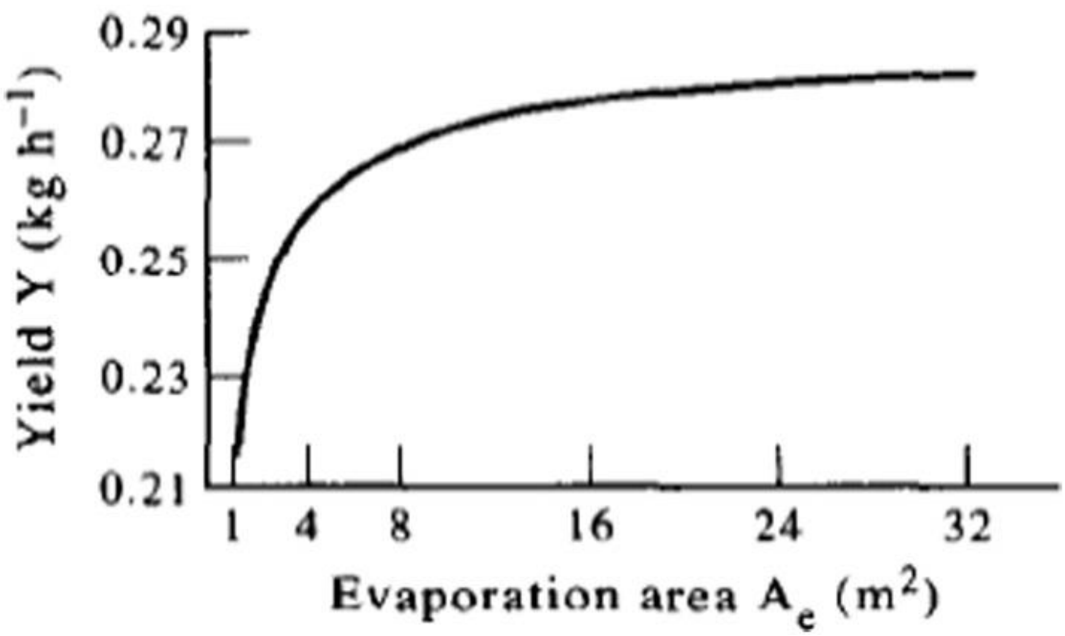

Figure 3. 12: the effect of the variation of evaporation area on distillation yield [28]

The **water deepness** is inversely proportional to the still heat. The maximum yield has been at minimum water depth. The optimum water depth is 4 cm, which was determined for an optimized SS production [28]. Constant thin layer of water depth may cause a dry spot, so a stepped water still to achieve the least deepness. Furthermore, as water depth increase in the SS basin the water volume and the water volumetric heat capacity increase.

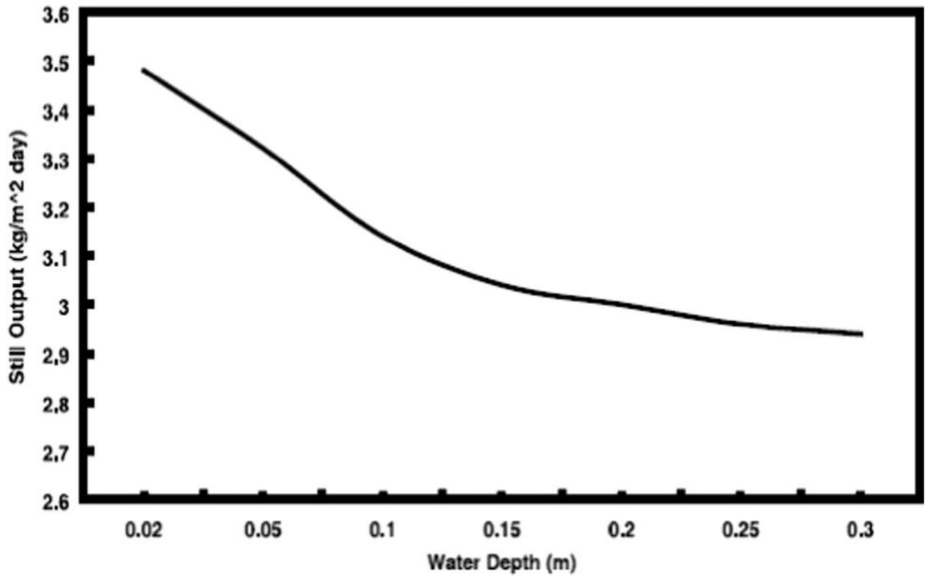

Figure 3. 13:The effect of water depth on the solar still productivity **[28]**

Insulation is an important physical parameter that plays an important role in preventing the release of thermal energy as waste heat from the sides of the basin.

3.3.3 Operational Parameters

Operational parameters, which include dust accumulation and system maintenance. Most of SS is generally fixed and there is no moving parts, so it does not require much maintenance. On the other hand, some of the designs have moving parts, such as rotating belt and fan, so maintenance is required regularly. In addition, cleaning continuously is necessary, due to its effect on the productivity.

Chapter Four: Methodology

Literature was served and a comparative study was done between many available designs that have been theoretically and experimentally suggested by other researchers, which are tabulated below (table 4.1)

Table 4. 1: Previous studies on various solar stills design and performance

<table>
<tr><th>Authors</th><th colspan="2">Productivity</th><th>System description</th><th>References</th></tr>
<tr><td>1. B.Jamil, et al</td><td colspan="2">4.186 L/m^2.day</td><td>Studied the effect of specific height at constant water depth and same basin area.</td><td>[31]</td></tr>
<tr><td>2. M. Abujazar, et al</td><td colspan="2">4.2 L/ m^2.day</td><td>A theoretical and experimental study on the efficiency of an inclined copper-stepped solar still</td><td>[32]</td></tr>
<tr><td>3. M. Al-harahsheh, et al</td><td colspan="2">4.3 L/m^2.day</td><td>Solar still enhanced by external collector and PCM was experimentally studied. 40% of productivity produced after sunset.</td><td>[33]</td></tr>
<tr><td>4. K. Rabhi,et al</td><td colspan="2">4.669 L/ m^2.day</td><td>The effect of pins fins absorber and condenser on single slope solar still.</td><td>[34]</td></tr>
<tr><td>5. S. Jaimes, et al</td><td colspan="2">2.68 L/m^2.day</td><td>The effect of water level and glass thickness on thermal efficiency of solar still.</td><td>[35]</td></tr>
<tr><td>6. H.S. Deshmukh, et al</td><td colspan="2">5-5.3 L/m^2.day</td><td>A storage unit were used with single basin solar still and study the effect of storage depth on productivity.</td><td>[36]</td></tr>
<tr><td rowspan="2">7. T. Elango, et al</td><td>Insulated Double basin, double slope</td><td>5.327 L/m^2 day</td><td rowspan="2">Single and double basin double slope glass stills were studied under insulated and un-insulated conditions for their production at various water depths of 1, 2, 3, 4 and 5 cm.</td><td rowspan="2">[37]</td></tr>
<tr><td>Insulated Single basin, double slope</td><td>4.401 L/m2 day</td></tr>
</table>

It is realized that the most available designs are batched solar stills, there are few theoretically suggested continuous designs, which were expected to give higher productivity. This was the motivation towards developing an applicable CSDU.

In this project's methodology, two main steps were followed:

4.1 Designing and building process.
4.2 Investigation of CSDU performance.

4.1 Designing and Building Process

The CSDU consists mainly from three main parts:

1. Basic Unit.
   - Rotating belt.
   - Galvanized steel basin with glass cover.
2. Secondary unit (Energy storage unit).
3. Condensation unit.

The following schematic (figure 4.1) shows all parts of CSDU.

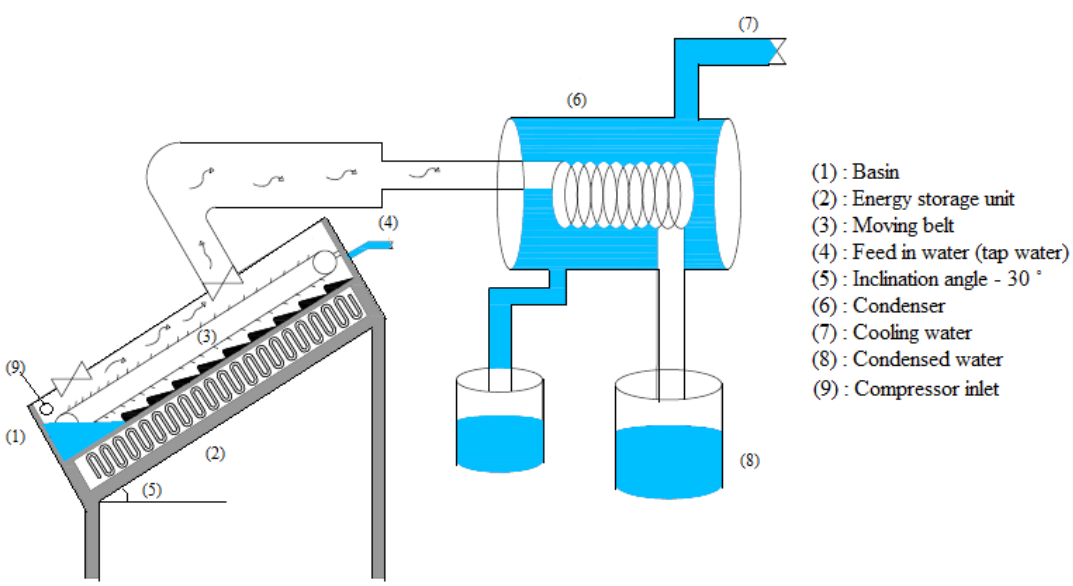

Figure 4. 1 schematic diagram of designed solar still drawn using AutoCAD

More described details about CSDU components are found in table 4.2

Table 4. 2: description about CSDU components

Component	Size	Material	Description	Purpose
Basin	1.8 m × 0.75 m × 0.3 m	Galvanized steel	Unit's sides are insulated with 0.04 m thickness of foam	The evaporation process takes place inside it.
Glass cover	(2 × 0.81 m) × 0.51 m	6 mm thickness	Solar heat gain coefficient = 0.8212 and U-value = 5.22 $W/m^2.K$ [29]	It allows the solar radiation to penetrate CSDU
Upper fan,	Diameter of 0.12 m	Plastic	Volumetric flow rate 95 m^3/h and	a suction fan to withdraw the produced vapor
Lower fan	Diameter of 0.15 m	Plastic	Volumetric flow rate 125 m^3/h.	Drive air over water surface to increase the evaporation and the driving force
Moving belt	2.7 m × 0.5 m	Canvas	With 70% absorptivity	To carry and distribute water by using fins. Also to increase the evaporation rate
fins	0.48 m × .035 m	Aluminum	0.5 cm height	Increasing the evaporation surface area
Mini air compressor	6 kg	Max pressure 8 BAR	Compressed air is introduced through a perforated tube	Enhancing the evaporation rate by introducing a compressed air
Motor	1 HP = 0.75 W	Metal	With a variable speed range (1.167 – 7) rpm	Driving the rotating belt with variation of speeds
Energy storage unit (Solar Water Heater)	1.8 m × 0.75 m × 0.1 m	Galvanized steel	The inner pipes are filled with PCM (Paraffin Wax) and the unit is filled with black sand.	PCM will store energy during the day, then release it during the night or in the absence of sun

For the basic unit, which is the upper part, a rubber belt was mounted on rolling cylinders in upward direction to carry and distribute the water placed at the bottom of the basin via black painted aluminum fins (0.5 cm height), which is attached to the surface of the belt along its width. The height of fins and basin were chosen according to the optimization that was done by Shadeed [38] The belt rotation will be controlled by motor of variable speeds, to allow investigating of the effect of belt speed on the evaporation.

The two circular suction fans of 0.12 m diameter were fixed on the glass surface. The lower fan drives air over the water surface enhancing turbulence flow, which in term increase the heat and mass transfer. The upper fan used as a suction fan to remove the air and water vapor from the basin to an external condenser which increase the mass transfer by maintaining the driving force high, and prevent water condensation on the glass surface that attenuate entry of solar radiation. The lower fan was replaced with a 0.15 m diameter fan to increase the driving force. Moreover, a perforated tube, to introduce compressed air, was fixed at the lower side of the basin, to increase the diving force inside the basin.

For the secondary unit, energy storage unit is a bottom tray, which is a solar water heater, contains copper tubes that was filled with paraffin wax as PCM to absorb heat during the day and release it through the night, the spaces between tubes was filled with Black sand. The external condenser was connected to the basin via outlet duct located at the top side of the basin.

Some modifications were made later such as; adding an insulation material called Vidoflex, which was used to cover the aluminum frame, because it was noticed that the aluminum frame caused significant heat losses as shown in (figure-4.2-b) this image was taken by a thermal camera, which forms an image using infrared radiation. The reduction in heat losses can be noticed in (figure 4.2-b), where insulation material was added. Vidoflex is an insulation material, which has a thermal coefficient range between (0.0308-0.036 $W/m^2.K$). The datasheet for vidoflex is included in appendix A figure A-1.

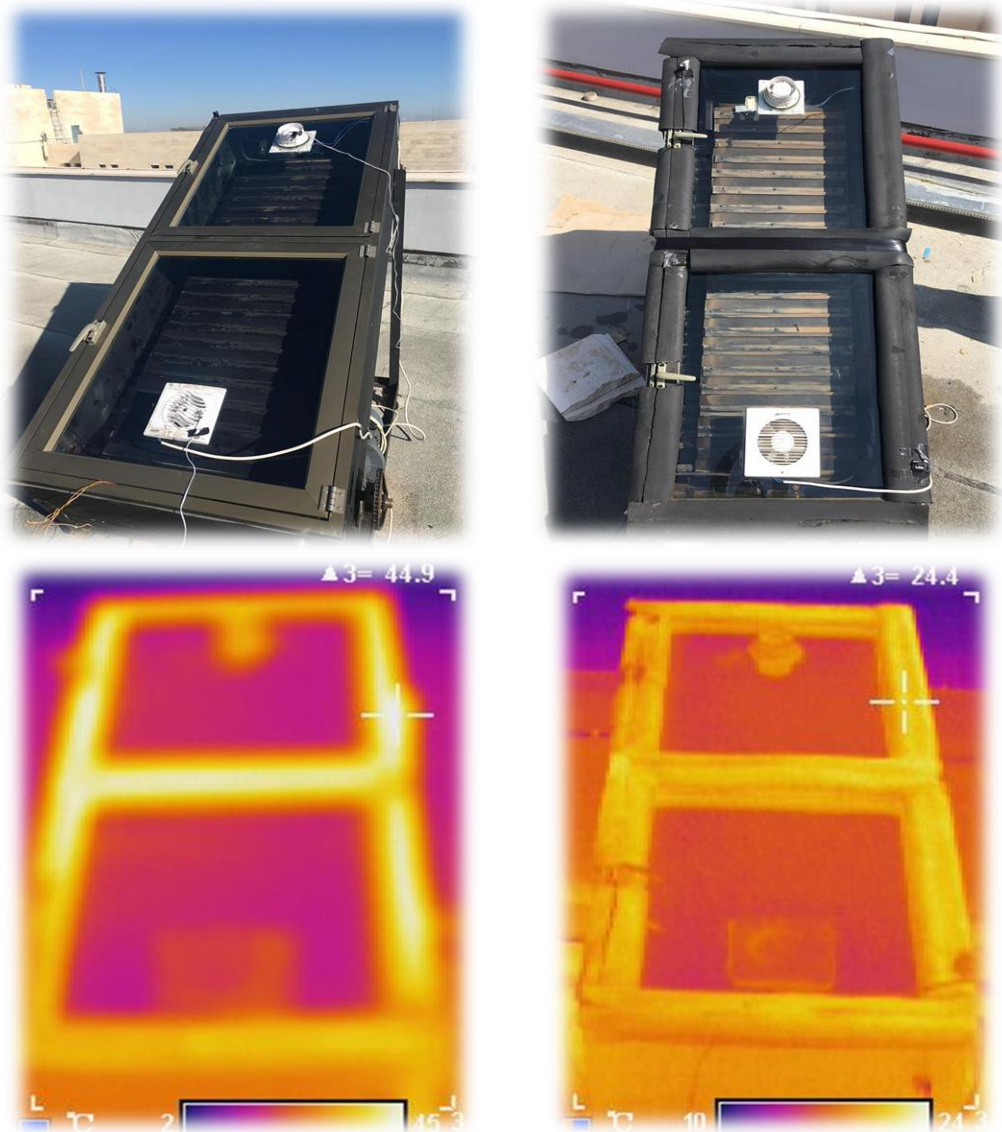

(a) **(b)**

Figure 4. 2: thermal camera pic for the unit (a): before insulation, (b): after insulation)

A 3D image for the CSDU is shown in figure 4.2 - (a) and a photograph for it after the insolation and condenser were added shown in figure 4.2 - (b)

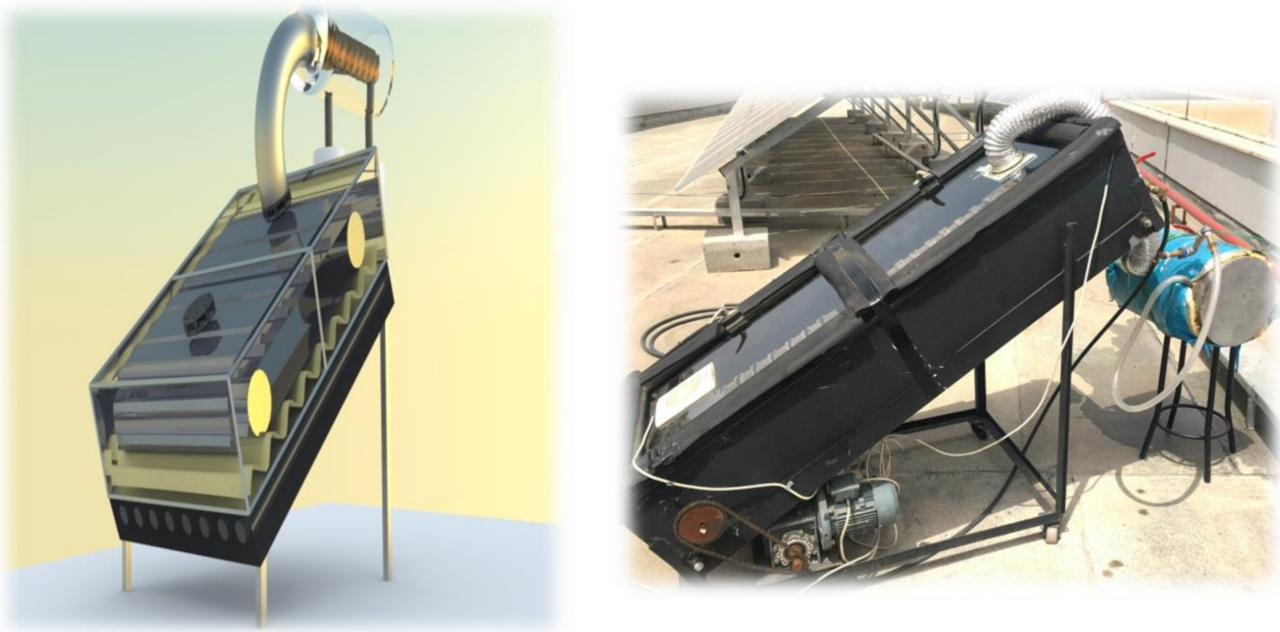

(a) (b)

Figure 4. 3: (a) - 3D image for CSDU, (b) - photograph for CSDU with condenser.

4.2 Investigation of CSDU Performance.

The CSDU was fixed on the engineering faculty's roof at An-Najah National University (ANNU) /Nablus. The unit fixed at 30˚ inclination to the south direction to collect the max solar radiation. Site location and weather conditions for Nablus are found in table 4.3, and a satellite photograph for ANNU is shown in figure-4.4.

Table 4. 3: Site location and weather conditions for Nablus

Site location	
Longitude	32°13'16"N
Latitude	35°15'15.98"E
Weather conditions	
Average ambient temperatures	13.3-22.3 C˚ [14]
Relative humidity	61 % [14]
Annual average daily solar radiation	5.4 kWh/day.m^2 [20]

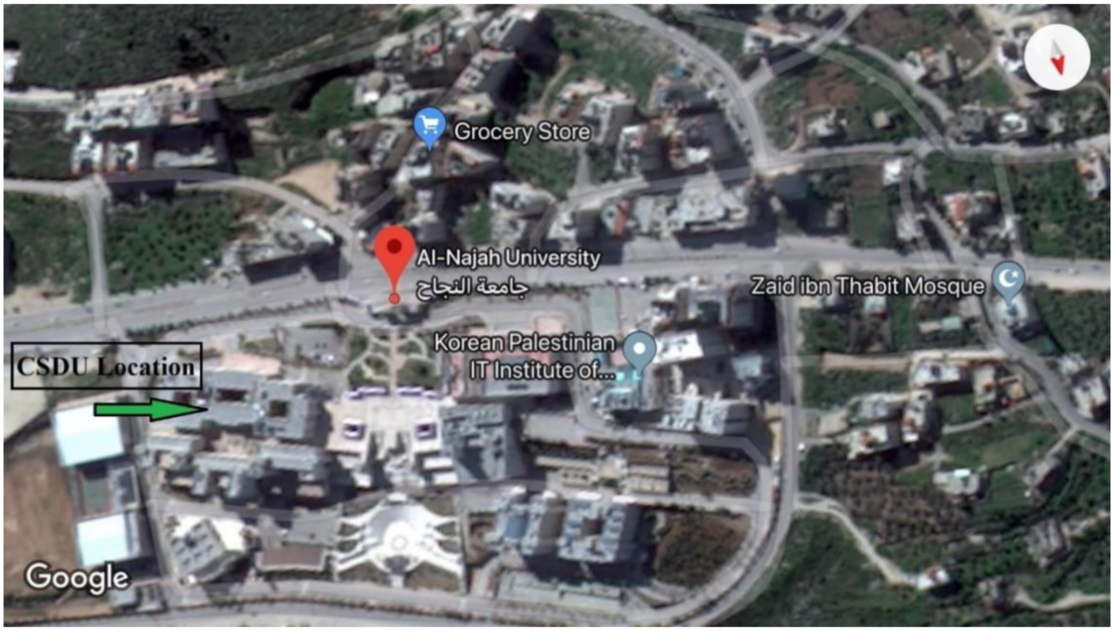

Figure 4. 4: A satellite photograph of ANNU, CSDU location is pointed with a green arrow [39].

Experimental studies were carried out during February, March and April of 2018. Generally, the following procedures were followed to operate the system unit:

- The measurement devices were installed
- 11-12 L of tap water was supplied to the basin to reach a height of 15.5-16 cm.
- Each experiment was performed approximately for 7-8 hours from 8:00 am to 4:00 pm.
- Lower and upper fans were operated at a volumetric flow rate 125 m^3/h and 95 m^3/h; respectively, where the rotating belt was running at speed 0.21 rpm.
- During the day, the Inlet and outlet temperature and relative humidity were measured at 10-second interval by two data loggers located at lower fan and upper fan. Solar radiation and basin water temperature were taken every 30 minutes manually.
- The evaporation rate was measured every 30 minutes by measuring the volume in the basin.
- At the end of the day, the remaining water (the unevaporated water) was drained at the end of the day from a tap, which is fixed at the bottom side of the basin.
- The effect of the weather conditions on the performance of CSDU were studied under different cases, which were clarified below:

These procedures were repeated in each case, but under different conditions. In order to study the effect of each case on the evaporation rate. Table 4.4 classifies each case according its operating mode and conditions.

Table 4. 4: operating modes for each case and their related conditions.

Operating conditions	Compressor	Upper fan	Lower fan	Rotating belt
Case-1	√	√	√	√
Case-2		√	√	√
Case-3			√	√
Case-4	√	√		√
Case-5		√		
Case-6		√		√

By looking at table 4.4, the marked rectangulars mean that parts are turned on, all cases were listed below:

Case-1: All parts are turned on.

Case-2: All parts are turned on except compressor.

Case-3: All parts are turned on except upper fan and compressor.

Case-4: All parts are turned on without lower fan.

Case-5: lower fan, compressor, and the rotating belt were turned off to study the effect of these parts on the productivity.

Case-6: lower fan, compressor was turned off to studies the effect of introduce air on the unit.

4.3 Measurements

The measured data were taken in two parts. For the first part, the data were collected manually every 30 minutes including, solar radiation, water temperature and water height (h). For the second group of data, it was measured using two data loggers to measure relative humidity and temperature for the inlet air (ambient air); the other one is used to measure relative humidity and temperature inside the basin.

In the first part, a TM-946 thermometer with two thermocouples were used to measure water temperature every half hour in two different places. The accuracy of thermocouples are ± 0.4 %. Solar radiation was measured every half hour using self-powered pyranometer SP-110-SS with an accuracy of ± 5 % (appendix A, figure A-2), which was connected to multi-meter. For water level in the basin, it was measured using a ruler and the evaporated vapor is calculated using the calibration curve stated in figure C.1, which can be found in Appendix B-2.

The second part of the collected data was monitored continuously and logged using a data logger for storing the temperature and relative humidity measurements. The logger is Zico Zi-9630 with an accuracy of ±3.5 % for relative humidity and ±2 % for temperature. The logger was programmed to measure data every 10 seconds. Then all of the stored data can be taken to an excel sheet to analyze. Data sheet is included in (appendix A, figure A-3).

Constrains

There are few constrains that bounded the designing and building process of the CSDU:

- To increase the solar absorption of the basin, belt and fins, it was painted with black color, which its absorb factor is 0.9.
- For the CSDU insulation, a foam (polyurethane) was chosen because of its low thermal conductivity (0.022 W/m.K), comparing with rock wool conductivity (0.044W/m.K)
- The thickness of the glass cover need to be as thin as it could be, in order to obtain the highest transmissivity . a glass with 6 mm and U-value5.778 (W/m^2 .K) was used.

Chapter Five: Results and Discussion

After building the CSDU, several experiments were conducted to investigate the productivity and the effect of different parameters. These experiments are summarized in this chapter.

5.1 Evaporation Rate Measurements

The productivity of CSDU along different weather conditions was measured and investigated. The results are represented by accumulative volume of evaporated water where the volume was measured on the whole day every 30 minutes; also it was measured by daily flux (L/m^2.day) the evaporation surface area was calculated in (appendix B-2).

5.1.1 Maximum and Minimum Evaporation Rate Achieved.

Productivity was measured along several days during February to April. The maximum and minimum values for accumulative volume of evaporated water are shown in figure-5.1. Refer to appendix C, table C-1 for hourly accumulative, weather parameters experimental data.

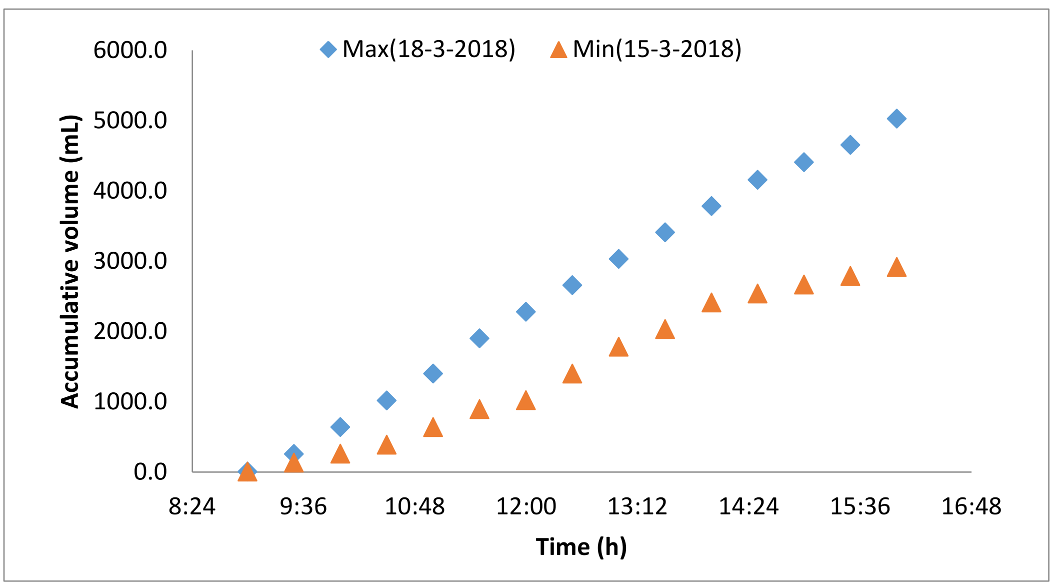

Figure 5. 1: The accumulative volume for Maximum and minimum cases.

The maximum and minimum evaporation fluxes achieved were 11.4 and 6.9 (liter/ m^2.day) on 18/3/2018 and 15/3/2018, respectively. These results were obtained at case-2 operating conditions (table-4.4). Where the accumulative volume achieved for maximum and minimum case were 5148.6 mL, 3164.1 mL, respectively. The cloudy and humid weather and lower ambient on 15/3/2018 affect highly the evaporation rate of the CSDU.

A summary of ambient conditions for these results are presented in table 5.1. The average evaporation flux was approximately 9.73 liter/ m^2.day, where the average productivity for conventional solar stills were (3-4) liter/ m^2.day [6], which is smaller than CSDU's productivity.

Table 5. 1: The ambient conditions for maximum and minimum evaporation rate.

	Evaporation flux (liter/ m^2.day)	**Solar Radiation (kWh/ m^2.day)**	**Ambient Temperature** (C^o)	**Relative Humidity (%)**	**Cloud (%)**
18/3/2018	**11.4**	**5.03**	**22.3**	**23.3**	**10.2**
15/3/2018	**6.9**	**4.11**	**17.77**	**40**	**33.5**

It was noticed from figure 5.1 and table 5.1 that a significant enhancement (39.5%) was achieved when the solar radiation was increased from 4.11 to 5.03. Thus, it is expected to reach a highest productivity value during summer season, where the maximum solar radiation reaches as high as 8.4 kWh/ m^2.day in June [20].

5.1.2 Comparison between Different Cases.

Several experiments were done under different conditions classified into many cases as mentioned in experimental process in (table-4.4). The effect of each case was investigated and discussed in the following sections at approximately average weather conditions illustrate in table-5.2 that presents also the hourly and daily evaporation flux for all experiments conducted for each case.

5.1.2.1 The effect of compressed air.

To study the effect of adding a compressor to the unit, two days were selected (5/3/2018 and 2/4/2018) to make the comparison at weather conditions were close together as shown in figure-5.2.

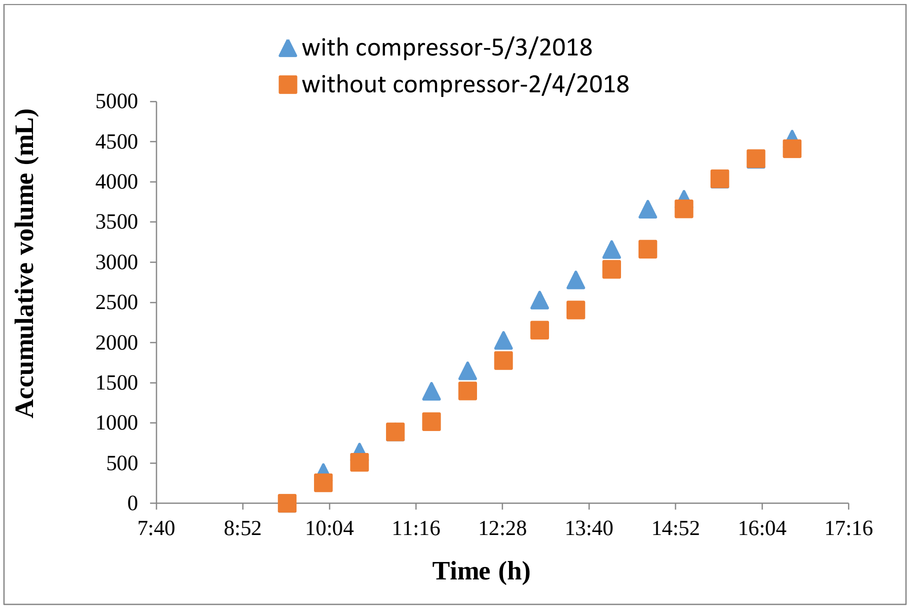

Figure 5. 2: Comparison between case-1 and case-2 at SR_{avg} = 5.37 kWh/ m^2.day, $T_{amb-avg}$ = 22.12 C° and RH_{avg} = 39.33%

It is expected that adding a compressor to introduce compressed air will be one of the great enhancements for the unit, because more dry air will be introduced. However, by comparing case-1 and case-2, switching off the compressor reduced the evaporation flux by 2.75 % under the same weather conditions, where the accumulative volumes for case-1 and case-2 were 4530.294mL, 4411.10 mL, respectively. The slight enhancement of compressor, which appears in figure 5.2, was due to low volumetric flow rate of the introduced air since the designed unit was large and needs larger compressor. The compressor is small and gives at most about 180 l/min at 8-bar pressure. So the experiments were continued without compressor to reduce the energy consumption.

5.1.2.2 The effect of upper fan:

The main functions for the upper fan is to withdraw the generated vapor, and accelerate the evaporation process. Also, to prevent water vapor from condensing on the glass cover and impeding the incident solar radiation. In this case, the upper fan is turned off to study its effect on the evaporation rate for 24, 27/3/2018 as appear in figure 5.3 by comparing this case with case-1 where the upper fan is turned on.

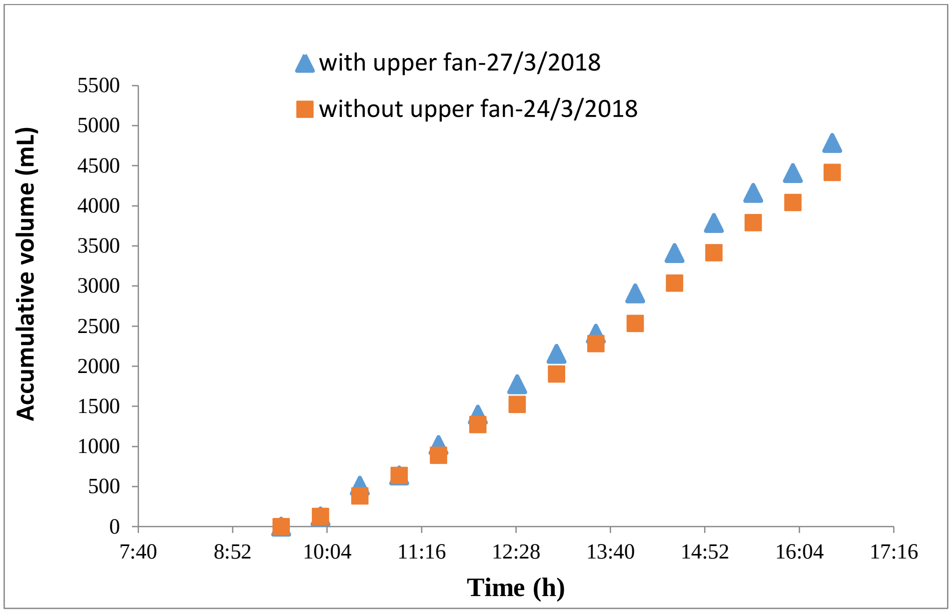

Figure 5. 3: Comparison between case-2 and case-3 at SR_{avg} = 5.878 kWh/ m^2.day, $T_{amb-avg}$ = 24.8 C° and RH_{avg} = 34%

The results show a low effect on the evaporation flux. The accumulative volume decreased from 4781.98 mL on 27/3/2018 and to 4665.98 mL on 24/4/2018. Where about 8.13% reduction in evaporation flux. It was noticed, during the experimental process, that without upper fan, the vapor will be condensed on glass surface.

5.1.2.3 The effect of lower fan

To investigate the influence of using lower fan, two days were selected at average solar radiation and ambient temperature and relative humidity: 5.457 kWh/ m^2.day, 28.88 C and 24.11%, respectively. The fan is switched off on 30/4/2018 and compared with 5/3/2018, when it was turned on as shown in figure-5.4.

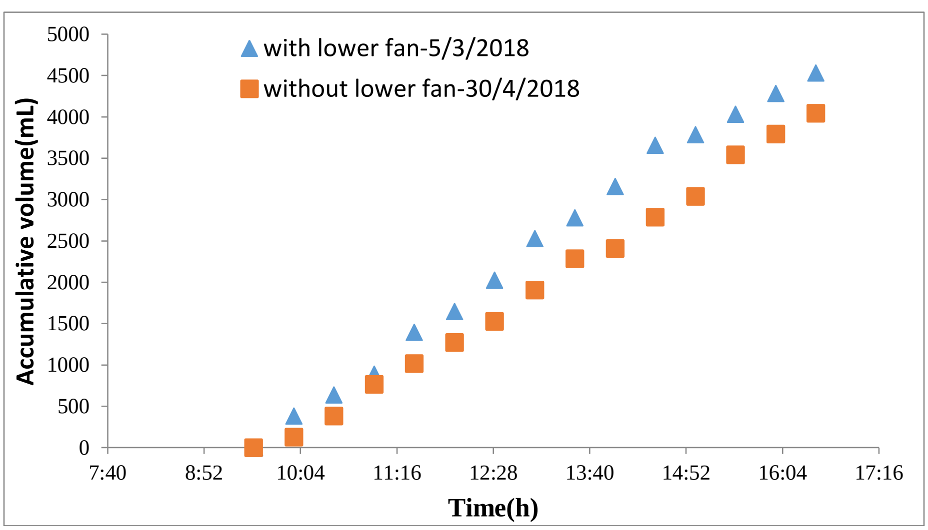

Figure 5. 4: Comparison between case-1 and case-4 at SR_{avg} = 5.457 kWh/ m^2.day, $T_{amb-avg}$ = 28.88 and RH_{avg} =24.11%

Theoretically, the lower fan will enhance the evaporation flux throughout increasing the mass transfer driving force and promote the heat transfer by forced convection. The experimental results match the theoretical expectations, where turning off the lower fan reducing the evaporation flux by 10.78%. It was 10.29 l/m^2.day with lower fan, while it was 9.753 l/m^2 day without using it. With accumulative volume 4530.294 mL, 4041.52 mL,respectively. However, it is clear from the deviation in figure-5.4 that the evaporation rate is relatively high in these two cases, since the compressor is used for both which promote the evaporation process.

5.1.2.4 The Effect of Operating Conditions.

To investigate the effect of all additive techniques to the batch design. The belt, lower fan and compressor were switched off on 21/3/2018, and compared with 5/3/2018 (figure-5.5) when all these devices were turned on. It should be mentioned that zero belt speed means that the evaporation occur just from the basin.

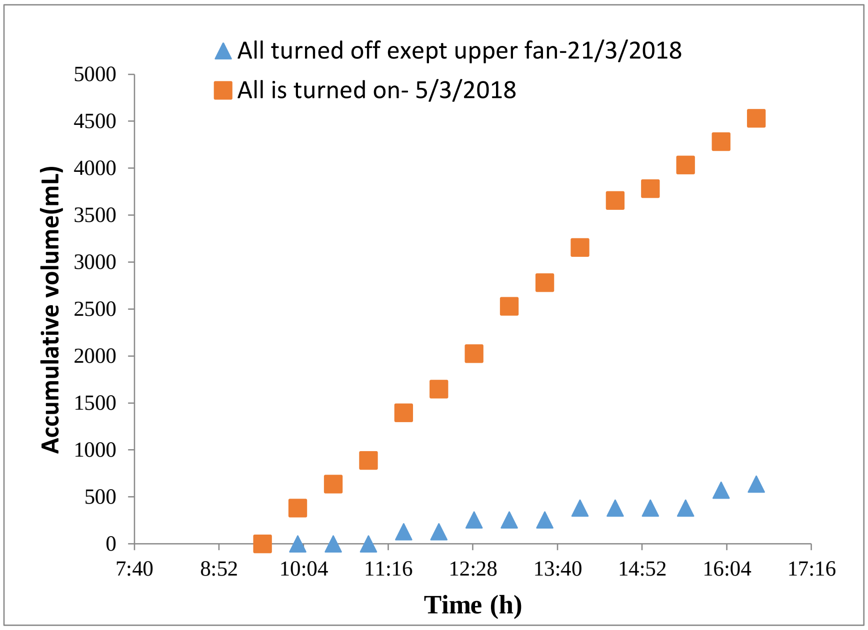

Figure 5. 5: Comparison between case-1 and case-5 at SR_{avg} = 6.27 kWh/m^2.day, $T_{amb\text{-}avg}$ = 25.8 C^o and RH_{avg} = 25.8%

Figure-5.5 shows a significant enhancement in the evaporation process when the belt, upper and lower fan and compressor were used (case-1) compared with this case when they turned off. The accumulative volume for case-1 is 4530.294mL and 635.86mL for case-5. The evaporation flux is reduced to approximately 1.3 (l/m^2.day). Which is considered very low compared to case-1 (10.29 l/m^2.day) about 87.3% enhancement. This means that all of them together make a significant improvement to the unit. It should be mention that upper fan kept turned on to prevent the condensation from returning back to the basin.

5.1.2.5 Overall comparison between all cases.

To facilitate the comparison, all cases were grouped, and the evaporation fluxes were measured and drawn in figure-5.6 under approximately the same weather conditions (SR_{avg} = 5.43 kWh/m^2.day, $T_{amb\text{-}avg}$ = 24.5 C^o, RH_{avg} = 32%).

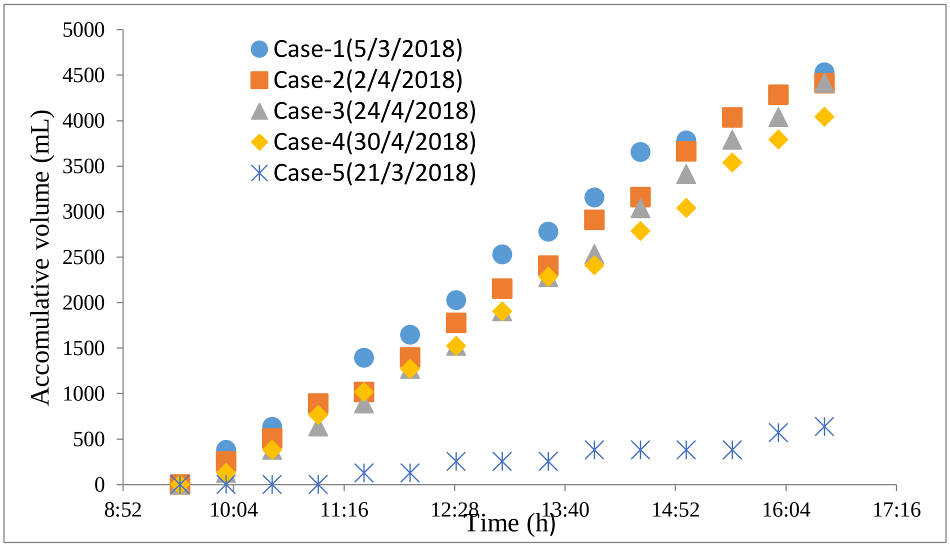

Figure 5. 6: Comparison between all cases that described in table-4.3

It is clear from figure 5.6 that the maximum evaporation flux among all mentioned cases was achieved in **case-1**, where rotating belt, fans and compressor were all turned on, it was 10.29 l/m^2.day. Which means that integrated of all these components enhance the evaporation rate. The accumulative volume for each case is shown in table-5.2. The reduction in evaporation flux for each comparison case is present in table 5.3. The hourly accumulative volume of evaporated water for all of these cases present in appendix C, table C-3.

Table 5. 2: Accumulative volume for all mentioned cases.

Day	5/3/2018	2/4/2018	24/4/2018	30/4/2018	21/3/2018
Case	Case-1	Case-2	Case-3	Case-4	Case-5
Accumulative volume (mL)	4530	4411	4413	4041	636

Table 5. 3: The reduction in evaporation flux for each comparison case.

Comparison case	Effect of compressor	Effect of upper fan	Effect of lower fan	Effect of all operational parts
Cases	Case-1 and 2	Case-2 and 3	Case-4 and 1	Case-5 and 1
Reduction in evaporation flux ($L/m^2.day$)	0.265	0.562	1.111	8.995

5.1.2.6 The effect of energy storage unit.

A paraffin wax as phase change material was used to enhance the productivity of CSDU. Which is a storage material using as a separate unit under the basin as an enhancement technique, where it absorbs heat during sunny days then releases it during the night and cloudy days. The influence of PCM on evaporation rate during the day of 24/4/2018 is noticed in figure-5.7.

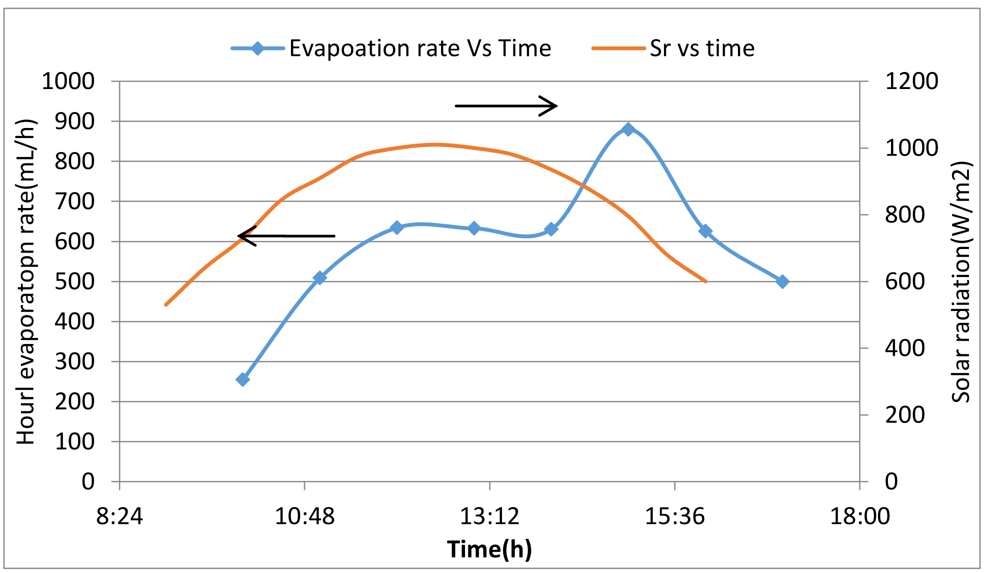

Figure 5. 7: Variation of hourly evaporation rate with solar radiation on 24/4/2018 at SR_{avg} = 5.835 $kWh/m^2.day$, $Tamb_{-avg}$ = 24.99 C° and RH_{avg} = 38%

Figure-5.7 shows the effect of PCM on the evaporation rate. It is reach its maximum value (880 mL) at 15:00 pm. Traditionally, while solar radiation starts decreasing the evaporation rate increases to reach its peak and that is the case in all conventional solar desalination unit without PCM. But in our case, when solar radiation reduces, paraffin wax start releases its heat to enhance the evaporation rate which explains the jump that occurred between 2 and 4 pm (refer to appendix C, table C-4 for hourly evaporation rate and solar radiation on 24/4/2018). It is expected that basin temperature reaches a value higher than the melting point of paraffin wax which is in range (48-52) C.

For more described and detailed data about each experiment, table 5.4 illustrate these data.

Table 5. 4: The evaporation fluxes at average weather conditions for all conducted experiments.

Case-1: Everything is on with compressor								
Operating hrs	Date	Evap.Rate	flux hourly	flux daily	Avg.SR	Avg.Tamb	Avg.RH	Avg.Cloud
7	5/3/2018	0.64718	1.470875	10.296	5.4	22.49	38.6	0
7	6/3/2018	0.55646	1.264675	8.8527	5.7	19.068	62	15.8889
Case-2: Everything is on without compreesor								
Operating hrs	Date	Evap.Rate	flux hourly	flux daily	Avg.SR	Avg.Tamb	Avg.RH	Avg.Cloud
7	12/3/2013	0.57632	1.309812	9.1687	4.43	16.7533	60.55	15.2222
7	15/3/2018	0.4338	0.985912	6.9014	4.11	17.1189	40	33.5333
7	18/3/2018	0.71779	1.631345	11.419	5.03	22.366	23.3	10.2
7	1/3/2018	0.61012	1.386643	9.7065	5.322	17	44	0
7	26/3/2018	0.64992	1.477091	10.34	5.796	24.26	25.44	0
7	27/3/2018	0.64797	1.472651	10.309	5.922	24.7	30.77	7.86
7	25/3/2018	0.62978	1.431312	10.019	4.043	17.33	47.11	3.2
7	2/4/2018	0.63054	1.433039	10.031	5.341	21.75	39.33	0
7	4/4/2018	0.61234	1.391676	9.7417	5.67	22.707	31.33	0
Case-3: Unit operate without upper fan and without compresser								
Operating hrs	Date	Evap.Rate	flux hourly	flux daily	Avg.SR	Avg.Tamb	Avg.RH	Avg.Cloud
7	13/3/2018	0.55814	1.268498	8.8795	4.785	18.6711	48.67	21.3889
7	14/3/2018	0.57666	1.310602	9.1742	5.733	18.8411	46.22	8
7	19/3/2018	0.66576	1.513101	10.592	5.553	28.35	17	0
7	19/4/2018	0.6116	1.389998	9.72999	5.221	23.4	41.22	0
7	23/4/2018	0.57736	1.312181	9.1853	5.721	19.995	37.3	0
7	24/4/2018	0.59522	1.352779	9.4695	5.835	24.99	38.08	4
Case-4: Unit operate without lower fan and with compresser								
Operating hrs	Date	Evap.Rate	flux hourly	flux daily	Avg.SR	Avg.Tamb	Avg.RH	Avg.Cloud
7	11/3/2018	0.32496	0.738546	5.1698	3.812	14.9489	67.22	68.6667
7	30/4/2018	0.57736	1.312181	9.1853	5.457	28.8863	24.11	3.44444
Case-5: Everything is off without compreesor with upper fan								
Operating hrs	Date	Evap.Rate	flux hourly	flux daily	Avg.SR	Avg.Tamb	Avg.RH	Avg.Cloud
7	21/3/2018	0.08177	0.18583	1.3008	6.272	22.99	25.8	0
7	22/3/2018	0.07265	0.165108	1.1558	5.346	25.998	16.86	2

This table summarizes the experimental results for all experiments conducted for each case at average ambient conditions. The hourly and daily achieved evaporation fluxes were present for each day.

5.2 Environmental parameters affecting solar still performance

The evaporation rate is highly influenced by environmental parameters. Several experiments were conducted and reported during February to April, at same operational conditions (case-2) and with belt speed 0.21 rpm. The studied ambient parameters include ambient temperature, relative humidity and solar radiation. In the following sections, the effect of each parameter will be described.

5.2.1 Effect of solar radiation.

The amount of solar intensity reaches the earth's surface significantly is affected by atmospheric conditions and geographical location according to the time of the day and season. Figure-5.8 shows the behavior of solar radiation during two different days (15/3/2018 and 27/3/2018) to investigate the relationship between solar radiation and the evaporation rate.

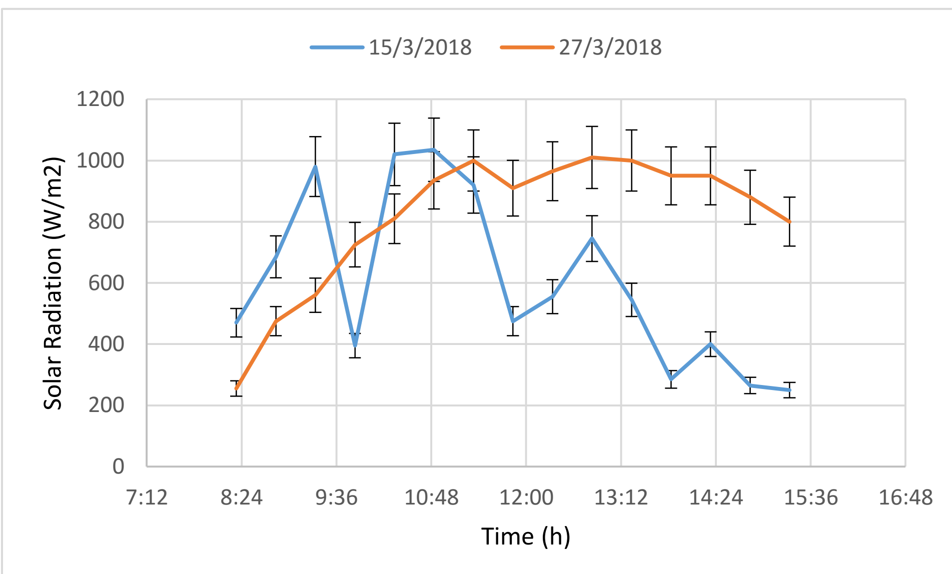

Figure 5. 8: Variation of solar intensity on two different days

Figure-5.8 shows the diurnal change of solar intensity for two different days. Although these data were collected in the same month, daily evaporation flux for 15/3/2018 was 6.901 L/m^2.day and for 27/5/2018 was 10.308 L/m^2.day. This is due to the oscillation, which is noticeable on 15/3/2018 that represents a cloudy day (total cloud cover reaches 33%), while on 27/3/2018, the total cloud cover was 7 %, which is considered as a clear day. The effect of solar radiation on accumulative volume is shown in figure-5.9 and 5.10 for 15/1/2018 and 27/3/2018, respectively. Their hourly accumulative volume and solar radiation presents in appendix C, table C-5.

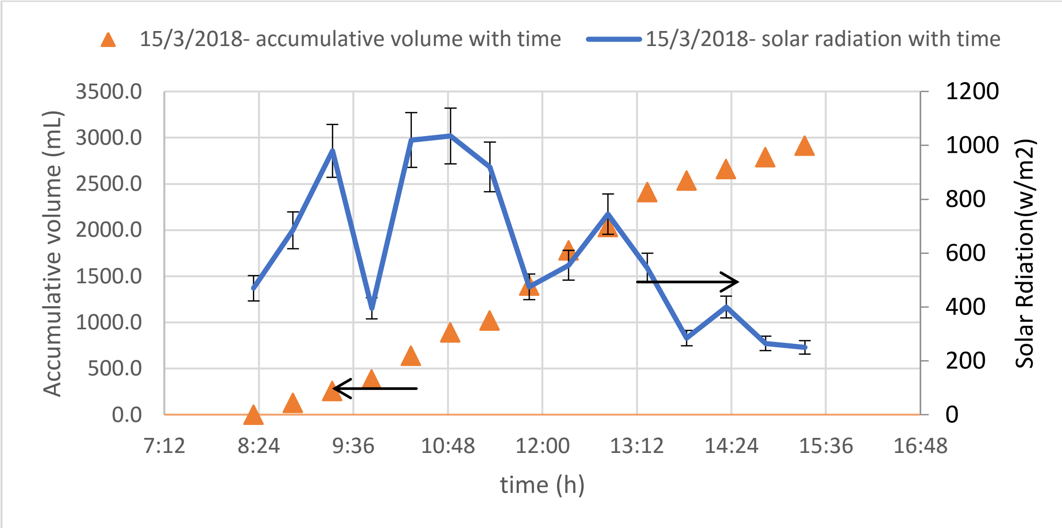

Figure 5. 9: The effect of solar radiation on unit's evaporation rate for 15/3/2018.

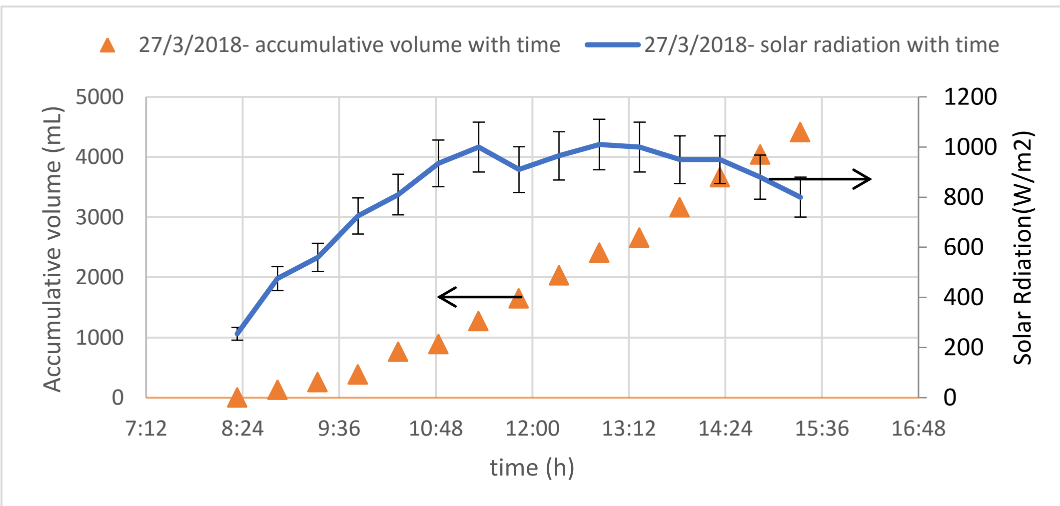

Figure 5. 10: The effect of solar radiation on unit's evaporation rate for 27/3/2018.

Significant effect of solar radiation on daily flux appears in figure-5.9 and 5.10, it show how daily flux increased on a clear day (27/3/2018) with average solar radiation = 5.92 kWh/m^2.day, it kept rising till the end in comparison with a cloudy day (15/3/2018) with solar radiation = 4.11 kWh/m^2.day, when solar radiation started decreasing (after 11:00 am) the rate of increment increasing for the accumulative volume reduced. A variation of 33.05% between daily fluxes for these days is obtained. Several experiments were carried out during days with different radiation intensity as shown in figure-5.11.

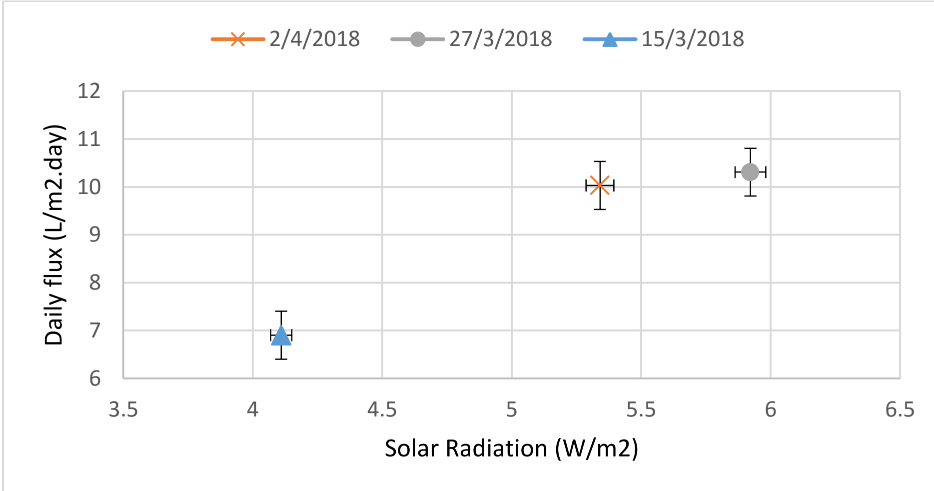

Figure 5. 11: Relationship between solar radiation and daily flux

Figure 5.11 shows a proportional relationship between solar radiation and daily flux, the average temperature and average relative humidity are 21.18 C° and 36.70 %; respectively. Table 5.3 shows daily flux and solar radiation for each day.

Table 5. 5: Daily flux and average solar radiation

Day	15/3/2018	2/4/2018	27/3/2018
Daily flux ($L/m^2.day$)	6.90	10.03	10.31
Solar radiation ($kWh.m^2.day$)	4.43	5.314	5.92

5.2.1 Effect of Temperature

Temperature plays an important role on affecting the unit's productivity. Temperature depends mainly on solar radiation, thus when solar radiation is relatively high during the day, ambient temperature will also be high. So this will affect the unit's evaporation flux positively, which can be noticed in figure-5.12. Figures 5.13 and 5.14 for the temperature pattern with solar radiation during two days (2/4/2018 and 4/4/2018) were plotted. Figure 5.15 shows the manner of temperatures for the ambient, basin and water on 2/4/2018.

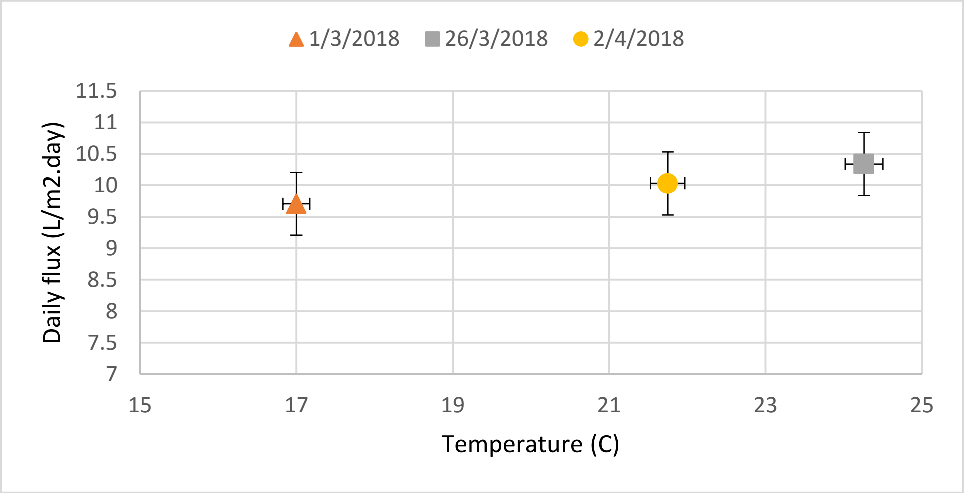

Figure 5. 12: Relationship between daily flux and temperature

A direct proportional relationship can be noticed in figure-5.11 between daily flux and temperature at average solar radiation = 5.486 kWh/m^2.day and average relative humidity = 36.26%. Table-5.4 shows daily flux and Ambient Temperature for each day.

Table 5. 6: Daily flux and Ambient Temperature.

Day	1/3/2018	2/4/2018	26/3/2018
Daily flux (L/m^2.day)	9.71	10.03	10.34
Ambient Temperature (C$^\circ$)	17.00	21.75	24.26

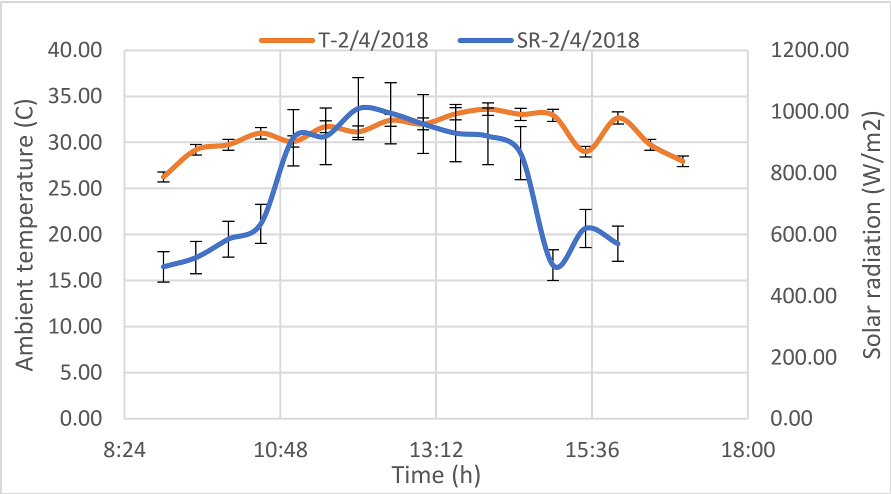

Figure 5. 13: Temperature variation with solar radiation for 2/4/2018

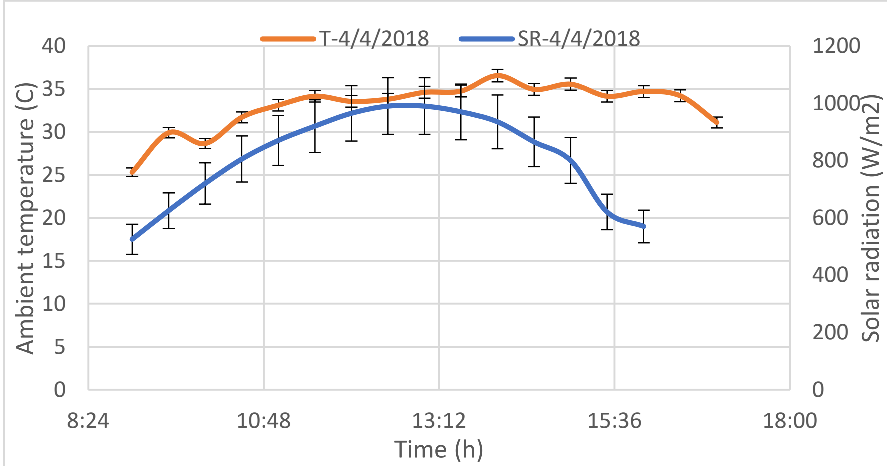

Figure 5. 14: Temperature variation with solar radiation for 4/4/2018

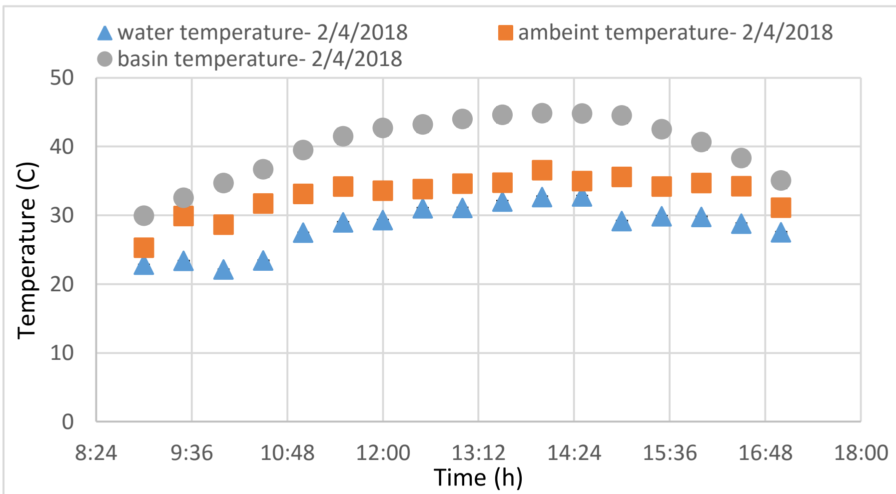

Figure 5. 15: Temperature variation between the inside and outside the basin in 2/4/2018.

As solar radiation penetrates glass cover, it will be trapped inside the basin. Thus will lead to increase the inside temperature and basin water temperature It is cleared from figure-5.15, that basin temperature reaches higher value than ambient temperature, due to greenhouse effect inside the basin. Also, basin temperature is higher than water temperature; this is due to that water has heat capacity higher than that for the basin.This indicates that CSDU has a good performance. Refer to appendix C, table C-6 for all collected data on 2, 4/4/2018.

5.2.3 The effect of relative humidity.

The relative humidity affects the productivity because it is affected indirectly by ambient temperature, which in turn affects the productivity according to the amount of water vapor presents in the dry air that entering the still unit. Figures-5.16 shows the trend of relative humidity versus temperature through 4/4/2018.

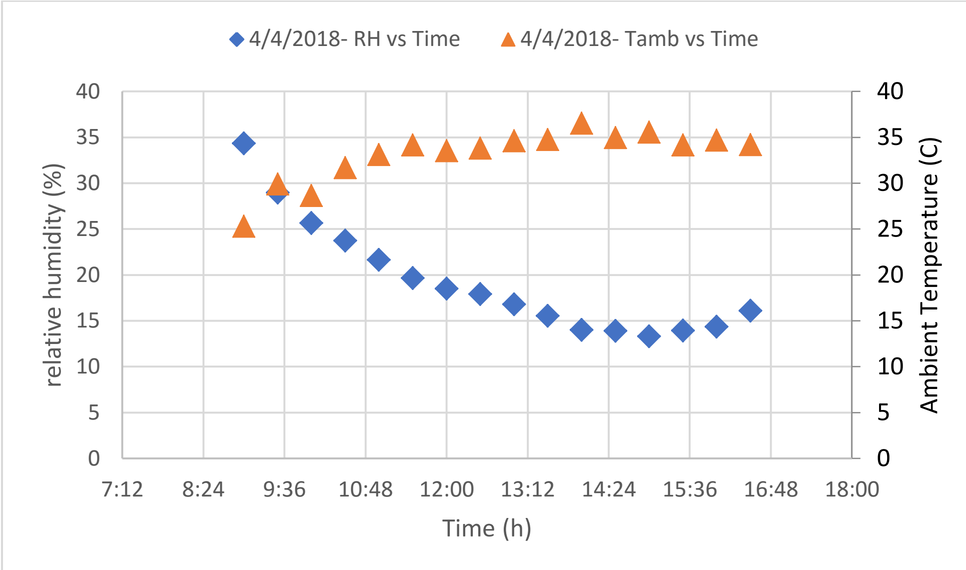

Figure 5. 16: Diurnal variation of relative humidity and ambient temperature on 4/4/2018

From figures-5.16, it is noticed that increasing of temperature causes a slight decreasing in relative humidity and vice versa and this reveal the inversely proportionality between them. Moreover, by comparing the average daily flux and relative humidity for different days, the productivity affected inversely as shown in figure-5.17.

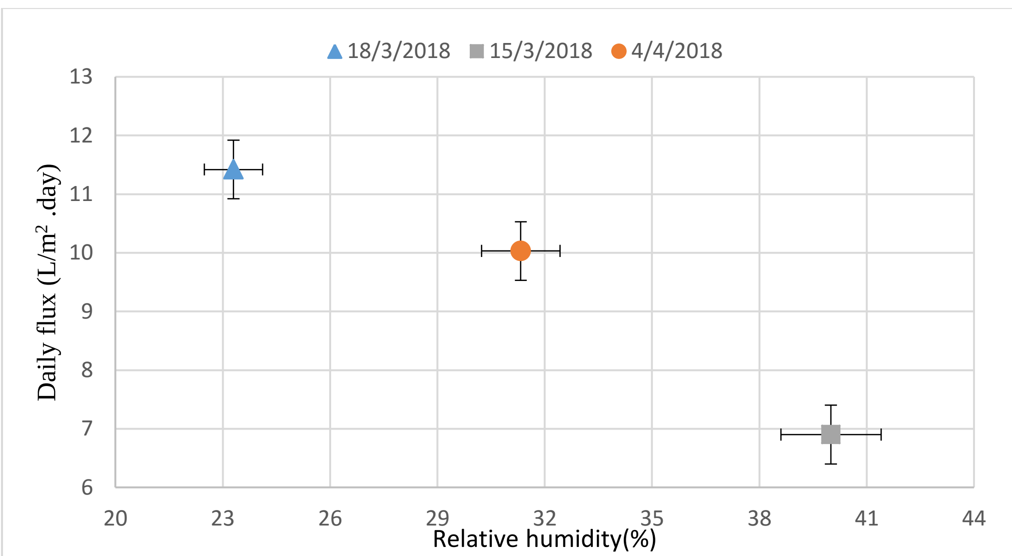

Figure 5. 17: Relationship between relative humidity and evaporation flux.

It is appearing from figure-5.17, that relative humidity has a negative effect on solar still evaporation flux, where the daily flux decreasing with increasing the relative humidity. This is due to the to the fact that, as the inlet relative humidity decrease, the mass transfer driving force increases which will increase the evaporation rate. Table 5.5 shows daily flux and relative humidity for each day

Table 5. 7: Daily flux and Relative Humidity

Day	18/3/2018	4/4/2018	15/3/2018
Daily flux (L/m^2.day)	11.42	10.03	6.90
Relative Humidity %	23.30	31.33	40.00

In order to study the effect of relative humidity on the evaporation rate of solar still, it was difficult to fix other parameters, so the daily evaporation flux is combined with solar radiation and relative humidity as shown in figure-5.18.

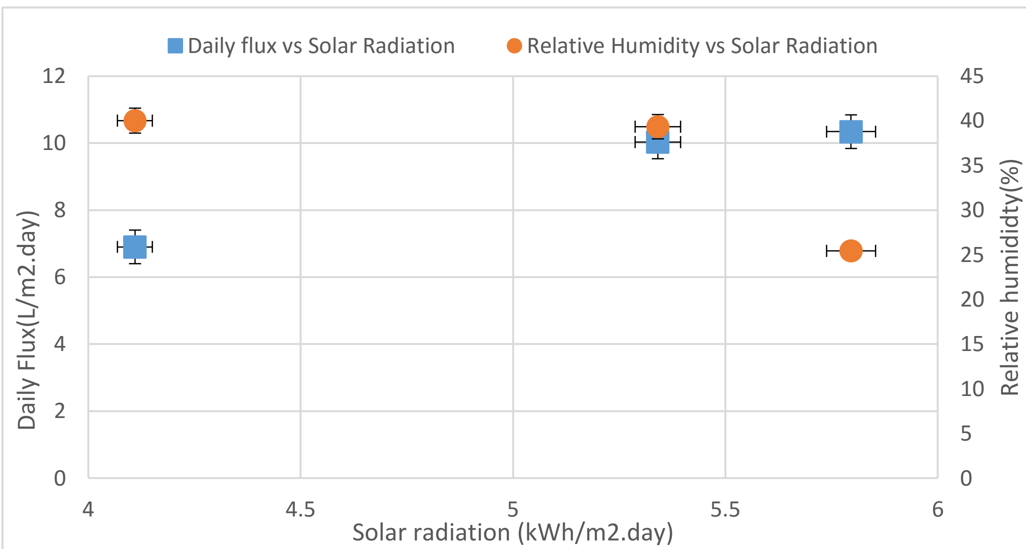

Figure 5. 18: Effect of solar radiation and relative humidity on Daily flux.

It was observed from the figure-5.18 that the increase of solar radiation caused a decreasing in relative humidity, which in terms affects the evaporation flux of CSDU. To get more convenient results, more data must be collected. It is recommended to find the formula that represents the change of flux with solar radiation. Table 5.6 shows daily flux, relative humidity and solar radiation for each day.

Table 5. 8: Daily flux, relative humidity and solar radiation for each day

Day	15/3/2018	2/4/2018	26/3/2018
Daily flux (L/m^2.day)	6.9	10.03	10.34
Relative Humidity %	40	39.33	25.44
Solar Radiation (kWh/m2.day)	4.11	5.34	5.79

For more assertive results, figure-5.19 shows the deviation between inlet and outlet relative humidity on 4/4/2018.

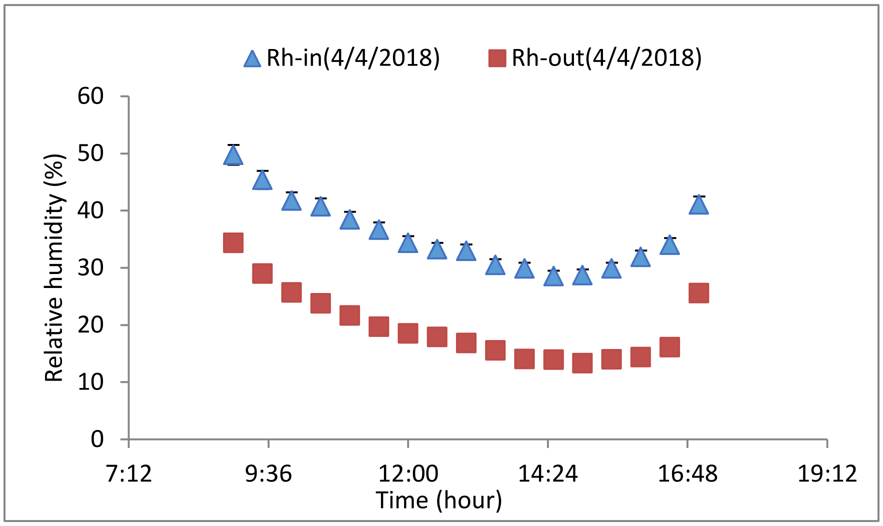

Figure 5. 19: Variation of inlet and outlet relative humidity on 4/4/2018.

The deviation was 16.1 between inlet and outlet relative humidity in figure-5.19 shows a good indication for the evaporation process inside the still. As produced vapor leaves the water surface, the humidity in the humid air inside the still will increase. However, entering a dry air with lower humidity ratio will allow the humid air to hold more vapor and increase the evaporation process.

- Importance of the project:

The proposed design is very simple compared with existing solar desalination units, Consumes very low energy. It should be mention that the unit's energy consumption was about 750 watt which is equivalent to operate about 7 incandescent lamps of 100 watt.

Figure 5. 20: Incandescent bulbs represent the energy consumption of CSDU

. Currently, a PV panel is planning to be added to the design, so it can provide the unit with its energy requirements, so it can be used everywhere, and it will be very useful in solving the water shortage problems in rare lands, in Gaza and many other suffered areas.

4. Conclusions and Recommendations.

Conclusions:

CSDU was constructed and fixed at the roof of engineering faculty at An-Najah University, Nablus. Its performance has been investigated under different weather conditions and operational parameters, for three months. The following points conclude all obtained results:

- The maximum evaporation flux achieved was 11.44 liter/m^2.day when the solar radiation was 5.03 kWh/ m^2.day and cloudiness15%. While the minimum evaporation flux among all experiments conducted through March and April was 6.9 liter/m^2.day when solar radiation was 4.11 kWh/ m^2.day and 33% cloudiness. the average evaporation flux obtained was 9.73 liter/m^2.day, which is considered high compared with the evaporation flux obtained using CSS (64.02 % enhancement).
- The effect of using moving belt and introduce air is very clear, a major enhancement of the flux it reaches up to 86% compared with the flux achieved with using the moving belt and the external air.
- The evaporation rate is directly affected by the weather conditions, specially; solar radiation, ambient temperature and relative humidity. The evaporation rate increases with increasing the solar radiation and temperature while it decreases when the relative humidity decreases.
- Although all experiments were conducted in cold or warm weather, the designed CSDU gave high evaporation rate. Thus it is expected to reach higher evaporation rate during summer season.

Recommendations

- To enhance the performance of the condenser, many parameters must be studied and optimized, such as; cooling water flow rate and temperature.
- The outlet of cooling water from the condenser can be fed directly to the basin to increase the energy integration.
- Preheating of feed water to the still basin using a preheating unit may significantly enhance the evaporation process.
- The aluminum frame used in the CSDU should be replaced with a wood frame to reduce the heat loss from the basin.
- It is recommended to replace the 6-mm glass cover with 3-mm one, because the thickness of transparent cover affect highly on the penetration of solar radiation.
- It is recommended to use a PV with storage batteries to provide the unit with its required energy during the day, so it can be used everywhere.
- It is recommended to find the formula that represents the change of flux with solar radiation

References

1. D. Dsilva Winfred Rufuss a, S.I., L. Suganthi b, P.A. Davies, Solar stills: A comprehensive review of designs, performance and material advances. Renewable and Sustainable Energy Reviews, 2016. 63: p. 464-496.

2. Deniz, E., Desalination Updates, Solar powered desalination, ed. R.Y. Ning. 2015: InTech. 37.

3. S.W. Sharshir, N.Y., Guilong Peng, A.E. Kabeel, Factors affecting solar stills productivity and improvement techniques: a detailed review. Applied Thermal Engineering, 2015. http://dx.doi.org/doi: 10.1016/j.applthermaleng.2015.11.041.

4. Hitesh N. Panchala, S.P., An extensive review on different design and climatic parameters to increase distillate output of solar still. Renewable and Sustainable Energy Reviews, 2016. 69: p. 750-758.

5. Ajay Kumar Kaviti n, A.Y., Amit Shukla, Inclined solar still designs: A review. Renewable and Sustainable Energy Reviews, 2015. 54(1364-0321): p. 429-451.

6. Ahsan, A., Fukuhara, T., Mass and heat transfer model of tubular solar still. Sol. Energy 2010. 84: p. 1147-1154.

7. T. Arunkumar, K.V., Amimul Ahsan, R. Jayaprakash,and SanjayKumar, Experimental Study onVarious Solar Still Designs. International Scholarly Research Network, 2012. 2012: p. 10.

8. Hitesh Panchal□, I.M., Various methods applied to solar still for enhancement of distillate output. Desalination, 2017. 415: p. 76-89.

9. A.A. Al-Karaghoulia, W.E.A., Experimental comparative study of the performances of single and double basin solar-stills. Applied Energy, 2004. 77: p. 317-325.

10. Z.M. Omaraa, A.S. Abdullah b, T. Dakrory, Improving the productivity of solar still by using water fan and wind turbine. Solar Energy, 2017. 147: p. 181-188.

11. El-Agouz, S.A., Experimental investigation of stepped solar still with continuous water circulation. Energy Conversion and Management, 2014. 86: p. 186-193.

12. S.A. El-Agouz ⇑, Y.A.F.E.-S., A.E. Kabeel, Performance evaluation of a continuous flow inclined solar still desalination system. Energy Conversion and Management, 2015. 101: p. 606-615.

13. Rajat Bharadwaj, D.S. and a.A. Mahapatra, Seawater desalination technologies. Int. J. Nuclear Desalination, 2008. 3(2): p. 151-159.

14. Organization, P.C.S., Palestine Statistical Yearbook. Vol. 17. 2016.

15. Desalination, M.-s.f.; Available from: http://www.swcc.gov.sa/english/AboutSWCC/DisinflationTechnology/Pages/MSF.aspx.

16. Distillation, M.E.; Available from: http://www.sidem-desalination.com/Process/Thermal-desalination-MED/MED/MED-TVC/.

17. Bradshaw, J. Nov 22, 2017]; Available from: https://www.oas.org/dsd/publications/unit/oea59e/ch20.htm.

18. Mohtada Sadrzadeh, T.M., Sea water desalination using electrodialysis. Desalination, 2008. 221: p. 440-447.

19. ; Available from: http://www.earthlyissues.com/solar.htm. [Online]

20. Adel Juaidi a, F.G.M.a., Imad H. Ibrik c, Francisco Manzano-Agugliaro, Renewable and Sustainable Energy Reviews. Renewable and Sustainable Energy Reviews, 2016. 65: p. 943–960.

21. Bapeshwararao VSV, S., TiwariGN, Transientanalysisofdoublebasin solar still. Energy Convers Manag, 1983. 23: p. 83-90.

22. Sabah A. Abdul-Wahab, Y.Y.A.-H., Performance evaluation of an inverted absorber solar still integrated with a refrigeration cycle and an inverted absorber solar still. Energy Sustain. Dev, 2013.

23. Nima Monghasemi, A.V., A review of solar chimney integrated systems for space heating and cooling application. Renewable and Sustainable Energy Reviews, 2017.

24. Sharma A, T.V., Chen C, Buddhi D., Review on thermal energy storage with phase change materials and applications. Renew Sustain Energy Rev, 2009. 13: p. 318-345.

25. Zakaria Haddada, Abla Chakera, Ahmed Rahmani, Improving the basin type solar still performances using a vertical rotating wick. Desalination, 2017. 418: p. 71-78.

26. M. El-Nagger, A.A.E.-S., M.R.I. Ramadan, S.A. Enein,, Experimental and theoretical performance of finned single effect solar still,. Desalin. Water Treat., 2016. 57: p. 17151–17166.

27. Y.A. Abakr, A.F.I., Theoretical and experimental investigation of a novel multistage evacuated solar still. J. Sol. Energy Eng., 2005. 127: p. 381–385.

28. Mohammed Shadi S. Abujazar , S.F. and A.R.R. , M.Z. Shahroma, The effects of design parameters on productivity performance of a solarstill for seawater desalination: A review. Desalination, 2016: p. 178–193.

29. K.A.R. Ismail*, J.R.H.q., U-values, optical and thermal coefficients of composite glass systems. Solar Energy Materials and Solar Cells, 1998. 52: p. 155—182.

30. Ali.F. Muftaha,b,□, K. Sopiana,□□, M.A. Alghoul, Performance of basin type stepped solar still enhanced with superior design concepts, Desalination, 2017, http://dx.doi.org/10.1016/j.desal.2017.07.017

31. Basharat Jamil □, Naiem Akhtar, Effect of specific height on the performance of a single slope solar still: An experimental study, Desalination, 2017, 414, 73-88

32. Mohammed Shadi S. Abujazara,□, S. Fatihaha,b, E.R. Lotfyc, A.E. Kabeeld, Suraya Sharile, Performance evaluation of inclined copper-stepped solar still in a wet tropical climate, Desalination, 2018, 425, 94-103

33. Mohammad Al-harahsheh a,⇑, Mousa Abu-Arabi a,b, Hasan Mousa a,c, Zobaidah Alzghoul, Solar desalination using solar still enhanced by external solar collector and PCM, Applied Thermal Engineering, 2018, 128, 1040, https://doi.org/10.1016/j.applthermaleng.2017.09.073

34. Kamel Rabhia,b, Rached Nciria,b,□, Faouzi Nasria,c, Chaouki Alia,d, Habib Ben Bacha, Experimental performance analysis of a modified single-basin single-slope solar still with pin fins absorber and condenser, Desalination, 2017, 416, 86-93

35. Alfonso Santos Jaimes1*, Emil Hernández Arroyo1, Zulma Y. Ramírez Jaimes2, Experimental Evaluation of a Single Slope Solar Still , Tecciencia, 2017, 12, 63-71, http://dx.doi.org/10.18180/tecciencia.2017.22.7

36. H.S. Deshmukh a,□, S.B. Thombre b, Solar distillation with single basin solar still using sensible heat storage materials, Desalination, 2017, 410, 91-98.

37. T. Elango, K. Kalidasa Murugavel, The effect of the water depth on the productivity for single and double basin double slope glass solar stills, Desalination, 2015, 359, 82-91. https://doi.org/10.1016/j.desal.2014.12.036

38. Shadeed, M., Solar drying and utilization of sludge produced at wastewater treatment, M. Sc. thesis, 2014, Chemical Engineering Department. Jordan University of Science and Technolgy.

39. https://maps.google.jo/maps?hl=ar&tab=wl. [Online] April 25, 2018

Appendices

Appendix A: Datasheets

Figure A.1: Datasheet for Vidoflex

vidoflex ANAVID

Vidoflex Sheets

Property	Value	Test method
Temperature range (°c)	+105 - 40(-)	
Density (kg/m³)	75 ⁻ 55	
Thermal conductivity λ W/(m*k)	0°c 0.037 10°c 0.038 20°c 0.039 30°c 0.039 40°c 0.040 W/ (m*k)	EN12667 or EN12939 for flat EN ISO 13787 for tubes
Water vapour diffusion resistance	μ >=10,000	EN 13469
Ozone resistance	No cracks	ASTM D 1171
U.V. resistance	No cracks	ASTM G 154
Water absorption	< 0.1 kg/m²	En 12086 For sheet & rolls En 13469 For tubes
Dimensional stability	Thickness Δε<3.0% Length & width Δε <2.0%	EN 1604
Fire behavior	Class 1 Class 0 V ; 3 ; 3	BS 476 Part 7 BS 476 Part 6 IIS 755 ת"י
CFC content	CFC & HCFC free	SFS 4190 Class 1

Figure A.2: Datasheet for Self-power Pyranometer SP-110-SS

	SP-110	SP-212	SP-214	SP-215	SP-230
Power Supply	Self-powered	5 to 24 V DC with a nominal current draw of 300 µA	5 to 36 V DC with a maximum current drain of 22 mA (2 mA quiescent current drain)	5.5 to 24 V DC with a nominal current draw of 300 µA	12 V DC for heater with a current draw of 15 mA
Output (sensitivity)	0.2 mV per W m^{-2}	2.0 mV per W m^{-2}	0.013 mA per W m^{-2}	4.0 mV per W m^{-2}	0.2 mV per W m^{-2}
Calibration Factor (reciprocal of output)	5.0 W m^{-2} per mV	0.5 W m^{-2} per mV	78 W m^{-2} per mA, 4.0 mA offset	0.25 W m^{-2} per mV	5.0 W m^{-2} per mV
Calibration Uncertainty	± 5 %				
Measurement Repeatability	Less than 1 %				
Long-term Drift	Less than 2 % per year				
Non-linearity	Less than 1 % up to 2000 W m^{-2}	Less than 1 % up to 1250 W m^{-2}			Less than 1 % up to 2000 W m^{-2}
Response Time	Less than 1 ms				
Field of View	180°				
Spectral Range	360 to 1120 nm				
Directional (Cosine) Response	± 5 % at 75° zenith angle				
Temperature Response	0.04 ± 0.04 % per C				
Operating Environment	-40 to 70 C; 0 to 100 % relative humidity; can be submerged in water up to depths of 30 m				
Dimensions	24 mm diameter, 28 mm height				
Mass (with 5 m of cable)	90 g		140 g	90 g	
Cable	5 m of shielded, twisted-pair wire; additional cable available in multiples of 5 m; santoprene rubber jacket (high water resistance, high UV stability, flexibility in cold conditions); pigtail lead wires				
Warranty	4 years against defects in materials and workmanship				

Figure A.3: Data sheet for Zico ZI-9630

SPECIFICATIONS

Relative Humidity	Overall Range	0 to 100%
	Accuracy (0 to 20 and 80 to 100%)	±5.0%
	Accuracy (20 to 40 and 60 to 80%)	±3.5%
	Accuracy(40 to 60%)	±3.0%
Temperature	Overall Range	-40 to 70℃ (-40 to 158℉)
	Accuracy(-40 to -10 and +40 to +70℃)	±2℃
	Accuracy(-10 to +40℃)	±1℃
	Accuracy (-40 to +14 and 104 to 158℉)	±3.6℉
	Accuracy(+14 to +104 ℉)	±1.8℉
Dew point Temperature	Overall Range	-40 to 70℃ (-40 to 158℉)
	Accuracy(25℃, 40 to 100%RH)	± 2.0 ℃ (±4.0℉)
Logging rate	Selectable sampling interval: From 2 seconds up to 24 hours	

Appendix B: Calculations

1. Water Volume Calculation and Calibration curve

The volume of water in the basin was calculated before starting the experimental cases, which is described as follows:

Water inside the basin takes the shape of Triangular Prisms, so to calculate the volume

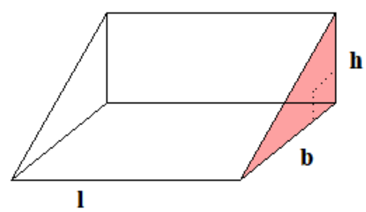

$V= 0.5 \times b \times h \times l$

h and b were measured by a fixed ruler, where l is the width of the unit (0.65 m)

For example: if h = 15 cm, b = 22 cm and l = 65 cm

$V = 0.5 \times 15 \times 22$

$\longrightarrow 10725\ cm^3 = 10.725\ L$

A calibration curve was done between the water height and the volume in order to create a simplified and easier way to calculate the volume for any height. As a result, figure below shows the relation between the water volume and its height, the equation is used to calculate the volume.

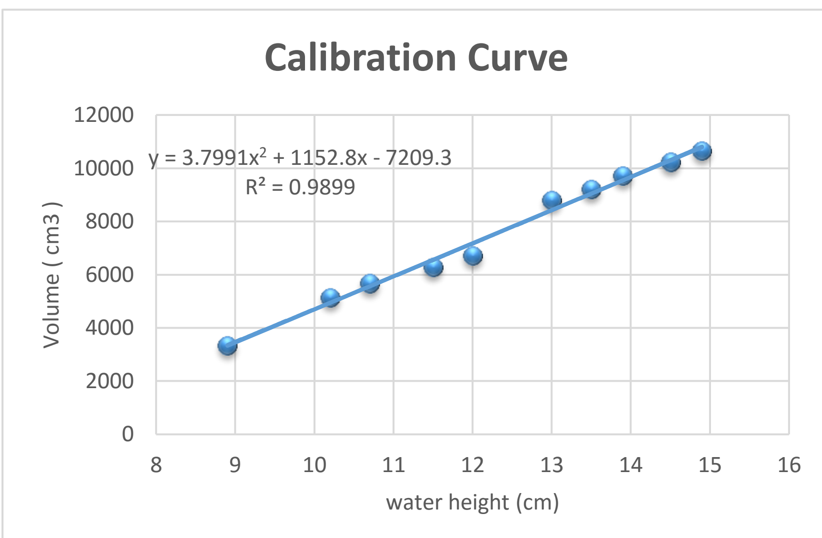

Figure C. 1: Calibration curve

2. Evaporation surface area

Water evaporations occur from three different locations areas; the basin, fins and the belt. Each area is calculated as follow:

1. Evaporation Surface Area for Basin:

Unit area from the inside = 65×170 cm^2

Maximum evaporation rate was on March 18th, 2018, evaporation rate = 0.5588 L/hour

H (maximum)= 15.6 cm, B= 22.7 cm,

C $\longrightarrow$ 27.379 cm

Maximum evaporation surface area= 65×27.379

$= 1779.635$ cm^2

H (minimum) = 11.5 cm, B= 17 cm,

C $\longrightarrow$ 20.524 cm

Minimum evaporation surface area= 65×20.524

$= 1334.06$ cm^2

Average evaporation surface area = $\frac{1779.635+1334.06}{2}$

$= 1556.8475$ cm^2

2. Evaporation Surface Area for Fins:

Fins surface area = 48.5×0.5 cm^2

Number of fins = 44 $\rightarrow\rightarrow$ top surface = 21 fins

Evaporation Surface area for fins = $21 \times 48.5 \times 0.5$

$= 509.25$ cm^2

3. Evaporation surface for belt:

Belt area = 49.5×270 cm^2

Evaporation surface area for the belt = (49.5 × 120 (top surface)) – (21 × 3.5 × 48.5)

$$= 2375.25\ cm^2$$

- Total evaporation surface area = 1556.8475 + 509.25 + 2375.25

$$= 4441.34\ cm^2 = 4.441\ L$$

Appendix C: Experimental Results

Table C-1: Results for experiments done on 15, 18 /3/2018 for minimum and maximum evaporation rate, respectively.

15/3/2018														
time	h(cm)	Volume in still (cm3)	Accumulative volume (mL)	solar (mV)	solar (w)	T-1 (water)	T-2 (water)	Tavg (water)	RH-in	T-1 in	T-1-out	RH-logger out	T-logger out	belt speed (rpm)
9:00	16	12208.07	0	137	685	29.8	20.2	25.0	66	15.9	22.4	68.8	33.7	0.21
9:30	15.9	12080.67	127.399129	196	980	34.5	22.4	28.5	61	17.4	25.3	61.2	36.5	0.21
10:00	15.8	11953.347	254.722276	79	395	34.6	23.7	29.2	56	18.5	26	56.6	35.8	0.21
10:30	15.6	11698.929	509.140624	204	1020	34.7	24.2	29.5	53	18.6	26.1	47.1	37.1	0.21
11:00	15.4	11444.815	763.255044	207	1035	31	24.4	27.7	54	18.3	24.5	42	40.5	0.21
11:30	15.3	11317.871	890.198281	184	920	36.9	24.5	30.7	52	19.1	27.1	44.3	38	0.21
12:00	15	10937.498	1270.5721	95	475	36	25.5	30.8	42	22.2	27.8	46.1	37.8	0.21
12:30	14.7	10557.808	1650.262081	111	555	33.6	25.5	29.6	41	22.6	26.6	49.6	33.2	0.21
13:00	14.5	10305.061	1903.008825	149	745	36.2	25.4	30.8	40	23.8	27.4	59	27.5	0.21
13:30	14.2	9926.5105	2281.559076	109	545	32	25	28.5	39	23.6	25.3	57.6	28.2	0.21
14:00	14.1	9800.4791	2407.590529	57	285	26.2	23	24.6	40	21.7	22.4	63.7	25.3	0.21
14:30	14	9674.5236	2533.546	80	400	25.1	20	22.6	47	21.3	22.3	63.1	20.9	0.21
15:00	13.7	9346.633	2861.436566	81	406	30	24	26.9	35	24.2	24.8	56.1	24.6	0.21
15:30	13.5	9094.907	3113.162582	73	366	29	24	26.7	33	24.9	24.8	56.3	23.3	0.21
16:00	13.3	8843.486	3364.583605	65	325	29	24	26.5	30	25.5	24.7	56.4	22.0	0.21
18/3/2018														
time	h(cm)	Volume in still (cm3)	Accumulative volume (mL)	solar (mV)	solar (w)	T-1 (water)	T-2 (water)	Tavg (water)	RH-in	T-1 in	T-1-out	RH-logger out	T-logger out	belt speed (rpm)
9:00	15.6	11698.929	0.0	153	765	25.5	23.3	24.4	32	19.7	27.5	28	41.9	0.21
9:30	15.4	11444.815	254.1	177	885	24.3	31	27.7	30	20	26	33.6	38.5	0.21
10:00	15.1	11064.213	634.7	180	900	25.1	25.4	25.3	23	25.9	26.7	34.5	37.7	0.21
10:30	14.8	10684.295	1014.6	191	955	26.3	26.1	26.2	18	29	28.2	34.2	40.9	0.21
11:00	14.5	10305.061	1393.9	219	1095	27.1	26.3	26.7	16	31.8	28.9	33.3	41.6	0.21
11:30	14.1	9800.4791	1898.4	175	875	27.6	23.2	25.4	16	31.5	28.7	34.3	41.2	0.21
12:00	13.8	9422.8406	2276.1	180	900	27.3	30.4	28.9	16	31.4	27.4	35.2	38.6	0.21
12:30	13.5	9045.886	2653.0	192	960	27.6	24.7	26.2	16	31.9	29.2	34.1	40.3	0.21
13:00	13.2	8669.6152	3029.3	178	890	28.8	25.4	27.1	14	33.1	29.7	30.6	42	0.21
13:30	12.9	8294.0282	3404.9	166	830	27.9	25.9	26.9	14	33.1	29.7	31.1	41.3	0.21
14:00	12.6	7919.1251	3779.8	108	540	26.5	25.6	26.1	14	33.1	29.7	34.9	36.4	0.21
14:30	12.3	7544.9058	4154.0	75	375	26.3	23.4	24.9	14	33.1	29.7	33.9	37	0.21
15:00	12.1	7295.8062	4403.1	72	360	24.3	18.9	21.6	14	33.1	29.7	36.6	33.8	0.21
15:30	11.9	7047.0106	4651.9	41	205	23	18.4	20.7	14	33.1	29.7	40.7	30.0	0.21
16:00	11.6	6674.3869	5024.5	49	245	23.1	21.7	22.4	14	33.1	29.7	44.2	27.9	0.21

Table C-2: Average experimental data for most conducted experiments for all cases.

Case-1: Everything is on with compressor								
Operating hrs	Date	Evap.Rate	flux hourly	flux daily	SR	Tamb	RH	Cloud
7	5/3/2018	0.6471848	1.4708747	10.2961	5.4	22.49	38.6	0
7	6/3/2018	0.5564568	1.2646746	8.85272	5.7	19.068	62	15.889
Case-2: Everything is on without compreesor								
Operating hrs	Date	Evap.Rate	flux hourly	flux daily	SR	Tamb	RH	Cloud
7	12/3/2013	0.5763175	1.3098124	9.16869	4.43	16.753	60.55	15.222
7	15/3/2018	0.4338012	0.9859117	6.90138	4.11	17.119	40	33.533
7	18/3/2018	0.7177917	1.6313448	11.4194	5.03	22.366	23.3	10.2
7	1/3/2018	0.610123	1.3866431	9.7065	5.322	17	44	0
7	26/3/2018	0.6499202	1.4770914	10.3396	5.796	24.26	25.44	0
7	27/3/2018	0.6479664	1.4726509	10.3086	5.922	24.7	30.77	7.86
7	25/3/2018	0.6297774	1.4313122	10.0192	4.043	17.33	47.11	3.2
7	2/4/2018	0.6305372	1.433039	10.0313	5.341	21.75	39.33	0
7	4/4/2018	0.6123373	1.3916757	9.74173	5.67	22.707	31.33	0
Case-3: Unit operate without upper fan and without compresser								
Operating hrs	Date	Evap.Rate	flux hourly	flux daily	SR	Tamb	RH-out	Cloud
7	13/3/2018	0.5581393	1.2684984	8.87949	4.785	18.671	48.667	21.389
7	14/3/2018	0.5766648	1.3106018	9.17421	5.733	18.841	46.222	8
7	19/3/2018	0.6657646	1.5131014	10.5917	5.553	28.35	17	0
7	19/4/2018	0.6115992	1.3899982	9.72999	5.221	23.4	41.22	0
7	23/4/2018	0.5773595	1.3121807	9.18526	5.721	19.995	37.296	0
7	24/4/2018	0.5952229	1.3527793	9.46945	5.835	24.99	38.081	4
Case-4: Unit operate without lower fan and with compresser								
Operating hrs	Date	Evap.Rate	flux hourly	flux daily	SR	Tamb	RH-out	Cloud
7	11/3/2018	0.3249601	0.7385457	5.16982	3.812	14.949	67.222	68.667
7	30/4/2018	0.577359497	1.312180675	9.1852647	5.457	28.88625	24.11111	3.444444
Case-5: Everything is off without compreesor with upper fan								
Operating hrs	Date	Evap.Rate	flux hourly	flux daily	SR	Tamb	RH-out	Cloud
7	21/3/2018	0.0817651	0.1858298	1.30081	6.272	22.99	25.8	0
7	22/3/2018	0.0726475	0.165108	1.15576	5.346	25.998	16.857	2

Table C-3: Hourly accumulative volume for compared cases.

	Effect of compressor (Case1,2)		Effect of upper fan (Case2,3)		Effect of lower fan (Case1,4)		Effect of operational parts (Case1,5)	
Time	5/3/2018 (with compressor)	2/4/2018 (without)	2/4/2018 (with upper fan)	24/4/2018 (without)	5/3/2018 (with lower fan)	30/4/2018 (without)	5/3/2018 (With)	21/3/2018 (Without)
9:30	0.000	0.000	0.000	0.000	0.000	0.000	0.000	0.000
10:00	381.286	254.570	254.570	127.399	381.286	127.475	381.286	0.000
10:30	635.096	508.837	508.837	381.969	635.096	382.197	635.096	0.000
11:00	888.603	889.666	889.666	636.236	888.603	763.711	888.603	0.000
11:30	1394.704	1016.458	1016.458	890.198	1394.704	1017.673	1394.704	127.323
12:00	1647.299	1396.376	1396.376	1270.572	1647.299	1271.332	1647.299	127.323
12:30	2025.621	1775.610	1775.610	1523.775	2025.621	1524.687	2025.621	254.570
13:00	2528.987	2154.160	2154.160	1903.009	2528.987	1904.149	2528.987	254.570
13:30	2780.214	2406.147	2406.147	2281.559	2780.214	2282.927	2780.214	254.570
14:00	3156.485	2909.209	2909.209	2533.546	3156.485	2409.034	3156.485	381.741
14:30	3657.116	3160.284	3160.284	3036.608	3657.116	2786.901	3657.116	381.741
15:00	3782.083	3661.523	3661.523	3413.107	3782.083	3038.432	3782.083	381.741
15:30	4031.791	4036.654	4036.654	3788.922	4031.791	3540.582	4031.791	381.741
16:00	4281.194	4286.361	4286.361	4039.085	4281.194	3791.201	4281.194	572.356
16:30	4530.294	4411.101	4411.101	4413.760	4530.294	4041.516	4530.294	635.856

Table C-4: Experimental results done on 24/4/2018

time	h(cm)	Volume in still (cm3)	Accumulative volume (mL)	Evaporation rate(mL)	solar (mV)	solar (w)	T-1 (water)	T-2 (water)	Tavg (water)	RH(in)-logger	T(in)-logger	RH(out)-logger	T(out)-logger	belt speed (rpm)
9:00	16.1	12335.54	0.00	0.00	106	530	25.2	35	30.1	26.3	29.8	58.8	32	0.21
9:30	16	12208.07	127.48	127.48	128	640	24.9	18.8	21.9	20.5	31.6	44.8	37.8	0.21
10:00	15.9	12080.67	254.87	127.40	146	730	26	18.8	22.4	20.3	33.1	42	40.5	0.21
10:30	15.7	11826.1	509.44	254.57	169	845	27.8	19.6	23.7	16	33.7	40.9	42.7	0.21
11:00	15.5	11571.83	763.71	254.27	182	910	29.3	20.6	25.0	14.8	33.8	39.2	44.8	0.21
11:30	15.3	11317.87	1017.67	253.96	195	975	30.5	39.8	35.2	14.3	35.3	39	46.1	0.21
12:00	15	10937.5	1398.05	380.37	200	1000	31	22	26.5	15	34.45	39.4	47.2	0.21
12:30	14.8	10684.29	1651.25	253.20	202	1010	31.6	22.6	27.1	14.2	36	40.2	47.6	0.21
13:00	14.5	10305.06	2030.48	379.23	200	1000	31.9	31.2	31.6	13.5	35.8	39.5	48.1	0.21
13:30	14.2	9926.511	2409.03	378.55	196	980	32.9	40.1	36.5	12.4	35	39	48.9	0.21
14:00	14	9674.524	2661.02	251.99	187	935	33.4	49.2	41.3	11.85	36	38	49.8	0.21
14:30	13.6	9171.462	3164.08	503.06	175	875	33.2	50.5	41.9	11.6	34	35.2	49.8	0.21
15:00	13.3	8794.963	3540.58	376.50	159	795	47.9	13.3	30.6	11.8	34.45	34.3	49.2	0.21
15:30	13	8419.148	3916.40	375.81	136	680	33.3	48.1	40.7	21.1	33.55	34	47.9	0.21
16:00	12.8	8168.985	4166.56	250.16	120	600	31.8	41.7	36.8	37.8	29.7	38.3	45.2	0.21

Table C-5: Experiments conducted on 15,27/3/2018 to study the effect of solar radiation.

15/3/2018						27/3/2018					
time	h(cm)	Volume in still (cm3)	Accumulative volume (mL)	solar (mV)	solar (w)	time	h(cm)	Volume in still (cm3)	Accumulative volume (mL)	solar (mV)	solar (w)
9:00	16	12208.1	0.00	137	685	9:00	15.9	12081	0.00	95	475
9:30	15.9	12080.7	127.40	196	980	9:30	15.8	11953	127.32	112	560
10:00	15.8	11953.3	254.72	79	395	10:00	15.7	11826	254.57	145	725
10:30	15.6	11698.9	509.14	204	1020	10:30	15.4	11445	635.86	162	810
11:00	15.4	11444.8	763.26	207	1035	11:00	15.3	11318	762.80	187	935
11:30	15.3	11317.9	890.20	184	920	11:30	15	10937	1143.17	200	1000
12:00	15	10937.5	1270.57	95	475	12:00	14.7	10558	1522.86	182	910
12:30	14.7	10557.8	1650.26	111	555	12:30	14.4	10179	1901.87	193	965
13:00	14.5	10305.1	1903.01	149	745	13:00	14.1	9800.5	2280.19	202	1010
13:30	14.2	9926.51	2281.56	109	545	13:30	13.9	9548.6	2532.03	200	1000
14:00	14.1	9800.48	2407.59	57	285	14:00	13.5	9045.9	3034.78	190	950
14:30	14	9674.52	2533.55	80	400	14:30	13.1	8544.3	3536.33	190	950
15:00	13.7	9346.63	2861.44	81	406	15:00	12.8	8169	3911.69	176	880
15:30	13.5	9094.91	3113.16	73	366	15:30	12.5	7794.3	4286.36	160	800
16:00	13.3	8843.49	3364.58	65	325	16:00	12.3	7544.9	4535.76	144	720

Table C-6: Results for experiments done on 2,4/4/2018 to study the effect of Ambient temperature and relative humidity.

2/4/2018													
time	h(cm)	Volume in still (cm3)	Accumulative volume (mL)	solar (mV)	solar (w)	T-1 (water)	T-2 (water)	Tavg (water)	RH(in)-logger	T(in)-logger	RH-logger out	T-logger out	belt speed (rpm)
9:00	16.00	12208.07	0.00	99.00	495.00	25.30	22.40	23.85	26.30	26.25	41.10	31.90	0.21
9:30	15.9	12080.67	127.399129	105	525	27.5	22.6	25.05	30.9	29.2	42.6	34.05	0.21
10:00	15.7	11826.1	381.969441	117	585	26.5	23	23	31.8	29.75	40.5	35.95	0.21
10:30	15.5	11571.834	636.235825	127	635	28.4	24.6	24.6	29.1	31	39.15	38.05	0.21
11:00	15.2	11191.004	1017.065536	183	915	30.9	26.1	28.5	31.1	30.1	39.2	39.1	0.21
11:30	15.1	11064.213	1143.856809	184	920	32.7	27.1	29.9	30.9	31.7	39	40.95	0.21
12:00	14.8	10684.295	1523.774736	202	1010	29.6	28.7	29.15	32.2	31.15	37.2	41.65	0.21
12:30	14.5	10305.061	1903.008825	199	995	32	29.2	30.6	31.2	32.4	38.65	42	0.21
13:00	14.2	9926.5105	2281.559076	192	960	29.9	29.5	29.7	31	32	38.3	42.05	0.21
13:30	14	9674.5236	2533.546	186	930	29.8	29.6	29.7	31.05	33.1	37.1	42.7	0.21
14:00	13.6	9171.4615	3036.608064	184	920	34.4	30.5	32.45	31.85	33.6	36	43.25	0.21
14:30	13.4	8920.3864	3287.683204	173	865	33	30	31.5	31.45	33.05	35.45	41.85	0.21
15:00	13	8419.1479	3788.9217	100	500	32	29.4	29.15	30.7	32.95	35.55	42.5	0.21
15:30	12.7	8044.0168	4164.052761	124	620	30.1	28.2	30.7	37.55	29	41.35	37.1	0.21
16:00	12.5	7794.3094	4413.760225	114	570	31.2	28.3	29.75	28.5	32.65	36.9	39.5	0.21
4/4/2018													
time	h(cm)	Volume in still (cm3)	Accumulative volume (mL)	solar (mV)	solar (w)	T-1 (water)	T-2 (water)	Tavg (water)	RH(in)-logger	T(in)-logger	RH-logger out	T-logger out	belt speed (rpm)
9:00	15.9	12080.67	0.00	105	525	23.6	22	22.8	34.35	25.3	49.75	29.95	0.21
9:30	15.8	11953.347	127.32	125	625	25.1	21.6	23.35	28.95	29.9	45.35	32.55	0.21
10:00	15.7	11826.1	254.57	144	720	26.3	22.1	22.1	25.65	28.65	41.75	34.7	0.21
10:30	15.5	11571.834	508.84	161	805	28.7	23.4	23.4	23.75	31.7	40.7	36.7	0.21
11:00	15.3	11317.871	762.80	174	870	30	24.9	27.45	21.65	33.1	38.45	39.5	0.21
11:30	15.1	11064.213	1016.46	184	920	31.8	26.1	28.95	19.65	34.15	36.65	41.5	0.21
12:00	14.9	10810.858	1269.81	193	965	30.4	28.2	29.3	18.5	33.55	34.35	42.7	0.21
12:30	14.5	10305.061	1775.61	198	990	33.5	28.5	31	17.9	33.8	33.2	43.2	0.21
13:00	14.2	9926.5105	2154.16	198	990	32.8	29.3	31.05	16.8	34.6	32.95	44	0.21
13:30	13.8	9422.8406	2657.83	194	970	34.1	29.9	32	15.55	34.75	30.45	44.6	0.21
14:00	13.6	9171.4615	2909.21	187	935	30.1	35.2	32.65	14	36.55	29.85	44.85	0.21
14:30	13	8419.1479	3661.52	173	865	35.3	30.2	32.75	13.9	34.95	28.5	44.8	0.21
15:00	12.8	8168.9845	3911.69	160	800	29.7	30	29.15	13.3	35.55	28.7	44.5	0.21
15:30	12.7	8044.0168	4036.65	124	620	30.1	28.2	29.85	13.95	34.15	29.85	42.5	0.21
16:00	12.5	7794.3094	4286.36	114	570	31.2	28.3	29.75	14.35	34.7	31.9	40.65	0.21